Novel Molecular Mechanisms in the Pathophysiology of Human Atrial Fibrillation

Foad Alzoughool

Thesis submitted to the

Faculty of Graduate and Postdoctoral Studies

in partial fulfillment of the requirements

for the Doctorate in Philosophy degree in Cellular and Molecular Medicine

Department of Cellular and Molecular Medicine

Faculty of Medicine

University of Ottawa

ABSTRACT

Background

The autonomic nervous system (ANS) plays an important role in creating a vulnerability to atrial fibrillation in otherwise healthy and young individuals. This is commonly referred to as vagal atrial fibrillation. The ANS regulates the parasympathetic (vagal) tone of the heart via fast synaptic transmission of neural inputs into the cardiac neural ganglia, which surround the heart. The molecular mediators of fast synaptic transmission of neurons comprising these ganglia are nictotinic acetylcholine receptors (nAChRs), especially α3β4 and α3α5β4 subtypes, which bind acetylcholine and lead to rapid transmission of cholinergic signalling onto atrial myocardial tissue. This vagal signalling leads to altered electrical properties of the atria, specifically slowing of heart and shortening of tissue refractoriness, which in turn set up a vulnerable substrate for initiation of AF. In this research, we hypothesized that rare genetic variants in the molecular mediators of parasympathetic transmission to the heart may be present in some patients with AF, and imbue a hypersensitivity of vagal tone on the heart contributing to an increased vulnerability to arrhythmia. In a large cohort of other healthy patients with lone AF, we identified and functionally characterized rare genetic variants of both the neuronal nicotinic receptor β4 subunit gene (*CHRNB4*) and the neuronal nicotinic receptor chaperone gene, *Ric-3*.

Methods and Results

We comprehensively sequenced the CHRNB4 and Ric-3 genes in 315 patients with lone AF and identified 4 rare mutations in each gene, absent from 600 elderly (age > 70 years)

controls with no reported history of arrhythmia. Mutant or wild-type *CHRNB4* were co-expressed in heterologous HEK tsa-201 cells with the alpha-3 nicotinic receptor subunit (*CHRNA3*) cell and the functional response to acetylcholine and nicotine agonists was measured. For Ric-3, mutant or wild-type Ric-3 were co-expressed in HEK293 cells stably expressing α3α5β4 nAChRs. Mutations in CHRNB4 showed significant differences in biophysical function, including alterations in receptor current density and sensitivity in response to neuroligand. A unifying observation among 4 mutant receptors was a significant increase in macroscopic current as compared to wild-type channels following repetitive application of agonist, indicating loss of receptor desensitization. All 4 rare mutations in the *Ric-3* gene led to significant enhancement of both nAChR current and surface expression.

Conclusion

These observations are consistent with a gain-of-function in nAChR behavior secondary to the identified rare mutations in the *CHRNB4* and *Ric-3* genes, which suggest that genetic influences on autonomic tone may contribute to AF vulnerability.

Table of Contents

List of Tables

List of Figures

List of abbreviations

aBgtx	α-Bungarotoxin
ACH	Acetylcholine
AF	Atrial Fibrillation
ANF	Atrial Natriuretic Factor
ANS	Autonomic Nervous System
AP	Action Potential
APD	Action Potential Duration
ATP	Adenosine triphosphate
BaCl2	Barium chloride
bp	base pair
BSA	Bovine serum albumin
C6	Hexamethonium
Ca+2	Calcium
CaCl2	Calcium chloride
cAMP	Cyclic adenosine monophosphate
cDNA	Complementary deoxyribonucleic acid

cGMP	Cyclic guanosine monophosphate
CsCl	Cesium chloride
CsOH	Cesium hydroxide
C-terminal	Carboxyl-terminal
CuSO4	Cupric sulfate
DMPP	Dimethylphenylpiperazinium iodine
DMSO	Dimethyl sulfoxide
DNA	Deoxyribonucleic acid
dNTP	deoxyribonucleotide
ECFP	Enhanced Cyan Fluorescent Protein
ECG	Electrocardiogram
EGTA	ethylene glycol tetraacetic acid
ER	Endoplasmic Reticulum
ERP	Effective Refractory Period
EYFP	Enhanced Yellow Fluorescent Protein
FBS	Fetal Bovine Serum
GAPDH	Glyceraldehyde 3-phosphate dehydrogenase
G-418	Geneticin

$I_{Ca(L)}$	Inward Currents of Ca2+
I_{Na}	Inward current of sodium
IK_{Ach}	Ach dependent inwardly rectified K+ current
I_{k1}	inwardly rectifying K+ current
I_{ks}	Slow delayed rectifier potassium currents
I_{kr}	Rapid delayed rectifier K+ currents
I_{to}	transient outward K+ current
IP3	Inositol 1,4,5,-trisphosphate
KCl	Potassium chloride
kHz	Kilohertz
mAChRs	Muscarinic acetylcholine receptors
MgCl2	Magnesium chloride
mM	Millimolar
msec	Millisecond
mV	Millivolts
MΩ	Megaohms
NaCl	Sodium chloride

nAChRs	Nicotinic acetylcholine receptors
Na2CO3	sodium carbonate
NAD+	Nicotinamide adenine dinucleotide
NaOH	Sodium hydroxide
NIC	Nicotine
N-terminal	Amino-terminal
PBS	Phosphate buffered saline
PCR	Polymerase Chain Reaction
PKA	Protein kinase A
PKC	Protein kinase C
PKG	Protein kinase G
Ric-3	Resistant to inhibitors of cholinesterase
RNA	Ribonucleic acid
S.E.M.	Standard error of the mean
TFR	Transferrin Receptor
TM	Transmembrane domain
UTR	Untranslated region

WT	Wild-type

Acknowledgements

I would like to express my gratitude and appreciation to all those who gave me the possibility to complete this thesis. I cannot express enough thanks to my PhD supervisor, Dr. Micheal Gollob for his continued support and encouragement. His enthusiasm, inspiration, guidance, and great efforts have been very influential and helped me to learn and explain things concisely. Throughout my Ph.D. training period, he provided encouragement, sound advice, good teaching, good company, and even skating lessons which made the long winters much more fun than I was expecting. Without his guidance and consistent assistance, I wouldn't have been able to finish this dissertation.

I would like to express my deepest appreciation to my committee members, Dr. Erik Suuronen, Dr. Robert Beanlands, and Dr. James Van Huysse for their support, encouragement, stimulating suggestions, and wise advices that helped me organize my project.

Special thanks go to Petro Doroshenko for showing and teaching me different experimental techniques such as Calcium Image Technique and Patch clamping. Without him, a big part of this thesis would never have happened. I would also like to thank with much appreciation Dr. Qiuju Li for helping me in patching clamp techniques, both experiments and calculation parts. I would like to thank Vivian Franklin for showing me the Radioligand assay and Markwell Lower technique for protein assay.

My thanks go to my best graduate student friends, especially Naif Al-montashiri for his appreciated efforts showing western blot experiments and for helping me get through the difficult times, and for all the emotional support that I received during the time I spent with him. I am indebted to my colleagues for providing a stimulating and fun environment to learn and grow. I am grateful to Tamara Checkland, Isabelle Thibodeau, Matthew Borkovich, Majed Jambi, Shaheen Uppal, and Maryam Kamkar.

I would like to specially thank my parents, Satea and Easa Alzoughool, for their unlimited support and infinite love. I send my appreciation and respect to my brothers and sisters for caring about me and my educational progress.

Finally, to my beloved and supportive wife, Samar and my little daughters Salma and Alma who fill my life with joy and happiness. Your encouragement when the times got rough are much appreciated and your help and generous emotional support made my success visible.

I dedicate this thesis to the memory of my grandmother, Hanyah Al-Ayasreh

1. CHAPTER 1

LITERATURE REVIEW

1.5 Atrial Electrophysiology

Atrial fibrillation (AF) is a challenging arrhythmia to manage. Current pharmacotherapy is of modest efficacy and side effects are common. Interventional therapy in the form of catheter ablation may have significant complications and recurrences post-procedure are common. These limitations provide strong reasons to pursue novel and more effective treatments. To design novel therapeutic approaches, a clear understanding of the molecular mechanisms that may lead to atrial fibrillation is essential. It is necessary to have knowledge of the normal electrophysiology of the atrium and sino-atrial (SA) node, the ionic channels that determine the action potential of the atrium and SA node, their pharmacological properties, and in particular the role of the autonomic nervous system in modulating the electrical properties of the atria.

The action potential (AP) of the atrium consists of four phases, starting at phase 0 by inward current through the Na+ channel (encoded by the *SCN5A* gene). At this phase the atrial myocytes depolarize from the normal resting potential between -70mV and -80 mV to reach about +30mV. After this, the Na channels start to inactivate until the atrial cells return to their repolarized phase at about -60mV. (Pourrier, M., et al. 2003) This repolarization process depends on the activity of time dependent outward K+ currents, such as, I_{to}: a short-lasting outward current that represents phase1 of the action potential; $I_{kur:}$ which is the ultra rapid delayed rectifier current contributing to phases 1 and 2 of the

AP, and I_{kr} (rapid) and I_{ks}(slow) which are delayed rectifier currents that represent phase 3 of the AP. During the second phase of AP, I_{Ca} also contributes an inward current leading to a plateau phase of the AP (Pourrier, M., et al. 2003). The molecular contributors to the atrial AP are summarized in see in Figure 1.

Another important atrial K+ channel is the acetylcholine (ACH)-sensitive K+ channel GIRK (Kir3.1/3.3) that is activated in response to cholinergic signalling (ACH) as the end mediator of parasympathetic effects on the heart (Dobrev, D., et al. 2001). This current, denoted $I_{KACH,}$ causes rapid atrial repolarization and shortening of the Action Potential Duration (APD). This phenomenon of action potential shortening is synonymous with decreasing the effective refractory period of atrial tissue, and is a well-accepted pre-requisite for setting up an electrical substrate facilitating the electrical micro-reentry, which characterizes the electrical behaviour of the atrial tissue during AF (Nattel, S., et al. 2002; Pourrier, M., et al. 2003; Yeh, Y-H., et al. 2007; Markides, V., et al. 2003).

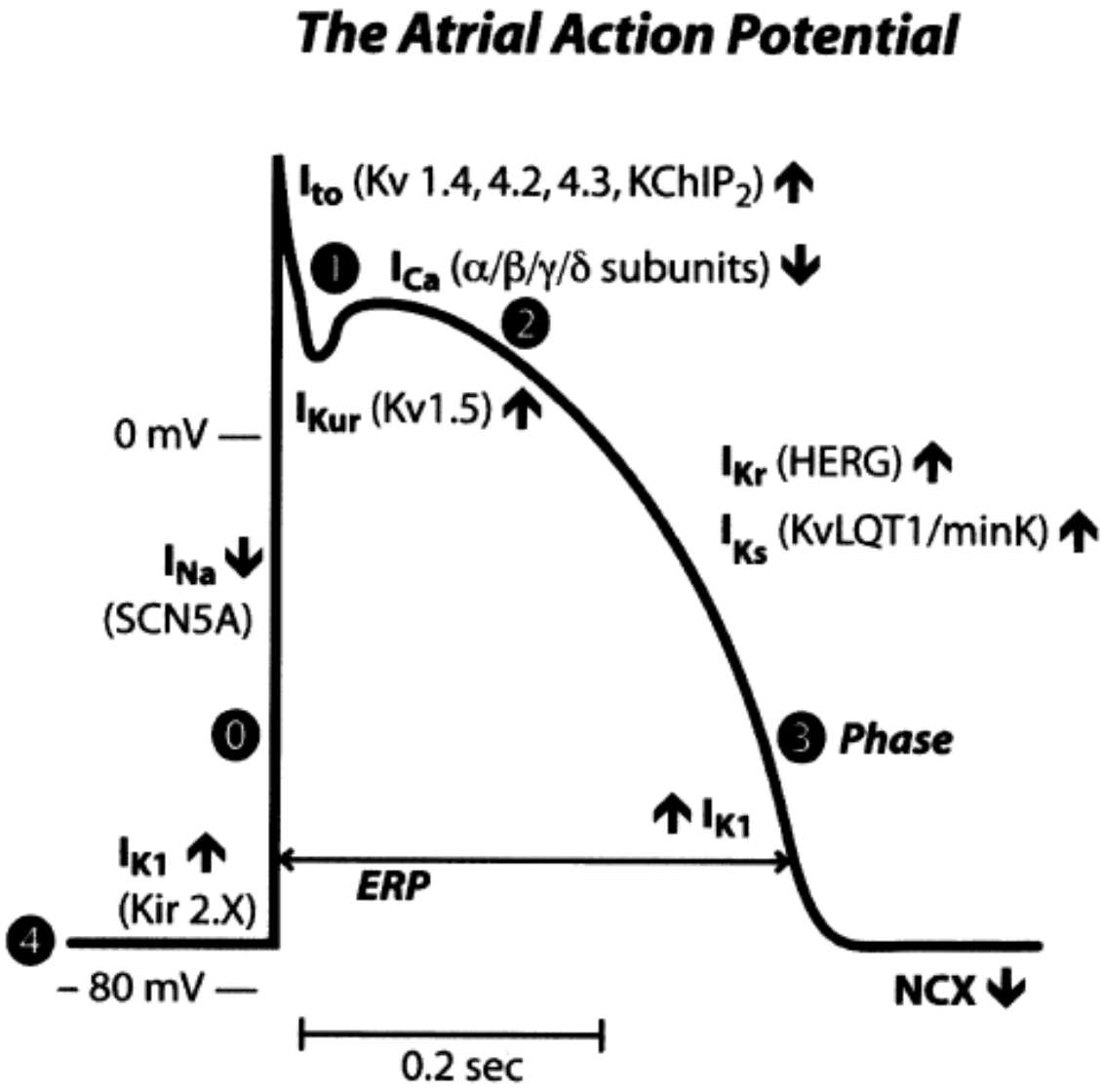

Fig. 1. A schematic representation of the atrial action potential with inward current (downward arrows) and outward currents (upward arrows). The molecular basis of each current is indicated in parentheses. Numbers within filled circles indicate the phases of the action potential.

(From Pourrier, M., et al. (2003). "Properties, expression and potential roles of cardiac K+ channel accessory subunits: MinK, MiRPs, KChIP, and KChAP." J Membr Biol 194(3): 141-152.)

1.2. Atrial Fibrillation

Atrial Fibrillation (AF) is the most common sustained cardiac arrhythmia and a leading cause of cardiovascular morbidity and mortality, particularly stroke (Ellinor, P. T., et al. 2003). AF is a growing health epidemic associated with a substantial clinical and economic burden (Braunwald, E. 1997). The lifetime risk of developing AF in individuals 40 years of age or older is approximately 1 in 4 (Lloyd-Jones, D. M., et al. 2004). Previously shown to be an independent risk factor for death (Benjamin, E. J., et al. 1998), AF is reported to correlate with a 5 time increased risk of stroke (Wolf, P. A., et al. 1991; Kannel, W. B., et al. 1991). AF is affects more than 6 million Americans, with an overall prevalence of 0.89% in persons younger than 60 years of age. It constitutes a growing epidemic in the aging population, the prevalence increasing with age, to 8% in those older than 80 years of age (McNamara, R. L., et al. 2003; Lloyd-Jones, D. M., et al. 2004). The incidence for women is about half that of men (McNamara, R. L., et al. 2003; Psaty, B. M., et al. 1997). Although AF may occur secondary to other conditions such as hyperthyroidism, vavular disease, left ventricular dysfunction, or hypertension, roughly 1/3 of patients have no obvious cause for their condition and are said to have lone AF (Gersh, B. J., et al. 1999). AF develops as a paroxysmal disorder characterized by rapid, irregular electrical activation of the atria and can be associated with palpitations, syncope, thromboembolic stroke, and congestive heart failure. Although lone AF is a common term, a genetic basis for AF is evident in population-based studies, and has now been well-established in both sporadic and familial cases (Roberts, J. D., et al. 2009, Thibodeau, I. L., et al. 2010; Mahida, S., et al. 2012).

Data from the Framingham Heart Study first demonstrated the genetic contribution to the arrhythmia, reporting that a parental history of AF is associated with a 1.85-fold increased risk of developing the arrhythmia in offspring. The risk of developing the arrhythmia in the presence of a sibling with lone AF is increased 70-fold in males and 34-fold in females (Fox, C. S., et al. 2004). The contribution of genetics to the development of AF in the absence of traditional risk factors such as hypertension and valvular heart disease, so called 'lone' or 'healthy heart' AF, appears to be much greater (Fox, C. S., et al. 2004; Ellinor, P. T., et al. 2005).

Human genetic investigations have identified AF–associated mutations in cardiac ion channels and gap junction proteins (Hodgson-Zingman, D. M., et al. 2008; Fox, C. S., et al. 2004; Gudbjartsson, D. F., et al. 2007; Brugada, R., et al. 1997; Darbar, D., et al. 2003; Chen, Y. H., et al. 2003; Olson, T. M., et al. 2005; Olson, T. M., et al. 2006; Gollob, M. H., et al. 2006; Thibodeau, I. L., et al. 2010). The genes associated with AF, coding mostly for ion channels are KCNQ1, KCNE2, KCNJ2, KCNE5, KCNA5, GJA1, *GJA5*, *NPPA*, and *SCNA5* (Roberts, J. D., et al. 2009). These mutations contribute to a minority of AF cases, leading researchers to believe that many other causative or contributory genes have yet been discovered (Darbar, D., et al. 2008).

Patients with AF frequently have symptoms of hemodynamic compromise, ranging from irregular palpitations to the more insidious feeling of malaise. They also have an increased risk for thromboembolism. Compared with age-matched controls, the relative risk for stroke in individuals with AF is increased 2- to 7-fold (McNamara, R. L., et al. 2003; Flegel, K. M., et al. 1987; Krahn, A. D., et al. 1995).

AF is characterized by an atrial rate of typically more than 400 per minute (Kockskamper, J., et al. 2002). It is the effect of this rapid atrial heart rate that leads to the major complications described above: cardiac dysfunction and thromboembolism (Nattel, S., et al. 2000). Thrombus formation during AF occurs predominantly in the left atrial appendage due to reduced contractility of the atria and associated blood stasis (Levy, S. 1998; Hart, R. G., et al. 2001). Left ventricular dysfunction may result due to AF since the rapid electrical heart of the atria is transmitted to the ventricles, albeit at a lower but still rapid rate (the atrio-ventricular node keeps the transmission of rapid atrial rate to the ventricles < 220 beats per minute).

The electrophysiology of Atrial Fibrillation:

At the cellular and molecular level, multiple ion channel changes have been shown to accompany and underlie AF in a number of experimental models. A common mechanism has been inferred in which changes in these ionic pathways contribute to decreased atrial action potential duration (APD) and subsequent atrial refractory period (Sampson, K. J., et al. 2008; Heist, E. K., et al. 2006). The surface electrocardiogram (ECG) of a patient with AF shows a rapid, irregular undulation of the baseline between QRS complexes. The intracardiac recordings show several types of atrial activity (Gavrilescu, S., et al. 1975). Figure (2) shows a comparison for normal ECG versus Atrial Fibrillation.

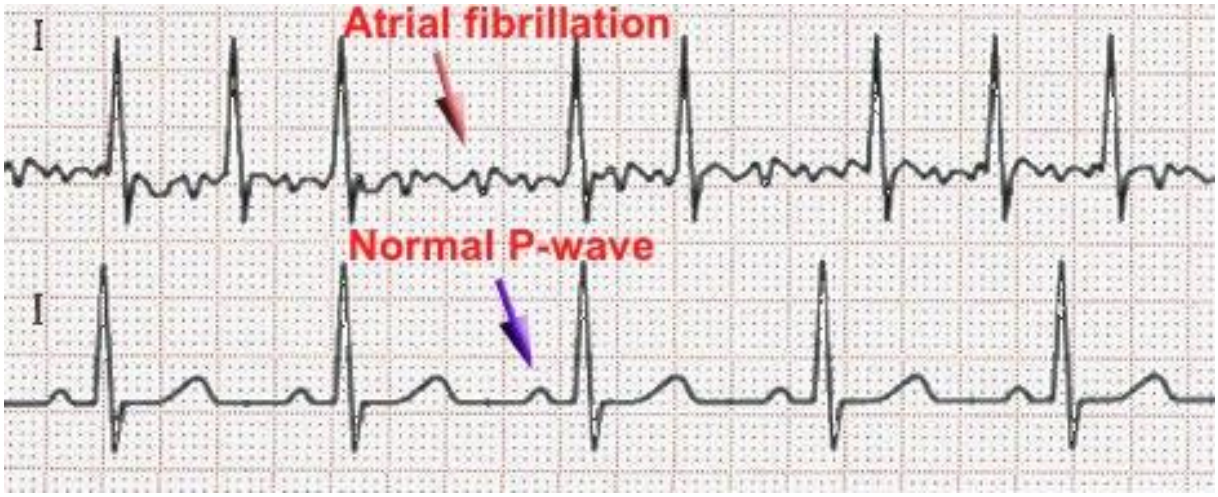

From http://www.goldbamboo.com/images/content/2411-400px-AF-ecg-atrial-fibrillation.jpg

Figure 2: ECG of atrial fibrillation (top) and normal sinus rhythm (bottom). The arrows indicate a P wave, which is lost in atrial fibrillation. The upper ECG show irregular R-R intervals due to irregular conduction of impulses to the ventricles.

Measurements of intracardiac electrograms during AF show that electrical activity may be completely disorganized and chaotic without isoelectric intervals, may show well-defined though irregular signals with an isoelectric baseline between them, or may exhibit regular flutter-like activity. These different patterns may coexist, so that one atrium may show flutter-like activity and the other a fibrillatory pattern (Leier, C. V., et al. 1980), or one pattern may merge into another over a short period of time (Wells, J. L., Jr., et al. 1978). Perpetuation of AF depends on the distance between depolarization wave fronts, the wavelength being short in relation to the size of atria. The shorter the wavelength, or larger the atria, the greater number of re-entry pathways can be accommodated. The wavelength depends on the speed of propagation of the action potential, and the duration of the subsequent refractory period (Smeets, J. L., et al. 1986). It is for these reasons that

changes in atrial tissue that result in a shorter refractory period (for example, modulated by parasympathetic tone) of the tissue promotes a substrate for AF. To express another way, a short refractory period mean that atrial myocardium is quickly repolarized and ready to propagate another action potential. In addition to refractory period, another electrical parameter important in setting up a substrate for AF or electrical re-entry is slow and inhomogeneous conduction velocity of depolarization through the atrial tissue. When relative differences exist in conduction velocity, a fast conducting region of tissue may be repolarized prior to a slow conducting adjacent region's depolarizing wavefront entering the region, and this slow wavefront may 're-enter' the already repolarized tissue. Thus not only effective refractoriness is relevant, but so too is the relative conduction properties of the tissue. The duration and uniformity of the signal-averaged P wave on the surface electrocardiogram may reflect atrial conduction velocities and the dispersion of refractoriness. Compared with control subjects, patients with paroxysmal AF have P waves that are longer, have more high-frequency content, and higher peak velocity change, suggesting slower and greater dispersion (due to heterogeneous pattern in tissue) of atrial conduction velocities (Stafford, P. J., et al. 1991).

Many factors may lead to changes in atrial tissue refractoriness and conduction velocity, and these changes may occur in a heterogeneous pattern through atrial tissue, again facilitating electrical re-entry. These factors include structural issues, like fibrosis that may develop from excessive strain on the atria from hypertension or valvular disease. Purely electrical phenomenon may also effect refractoriness and conduction, such as those induced by genetic alterations in specific ion channels (noted above) identified as genetic causes of AF. As briefly mentioned above and noted in more detail in the next

section, cholinergic signalling and release of ACH on atrial myocytes results in shortening the refractory period and conduction velocity, and infusion of acetyl-beta-methylcholine or acetylcholine itself may be used to precipitate AF in experimental animals (Burn, J. H. 1979). Inflammation may also alter ion channel function and result in patchy fibrosis. All of these structural, ion channel and neuropharmacology effects typically affect the atria in a heterogeneous pattern, setting up the substrate for electrical re-entry. However, from the standpoint of the development of AF and its prevention, the mechanisms underlying atrial repolarization is critical, especially in terms of the ionic currents involved in the action potential duration (APD) as well as the very important role of the autonomic nervous system (ANS), particularly parasympathetic component, in indirectly modulating these electrophysiological features.

1.3. Role of autonomic nervous system in AF

The ANS is recognized to play an important role in creating a vulnerability to AF. The first use of the term ‘vagal AF’ was by the French electrophysiologist Phillipe Coumel (Coumel, P., et al. 1978 and 1994). He reported that "vagal AF" usually occurs in young patients, ages 30–50 years, and more frequently in men who have no structural heart disease. It tends to occur post-prandially and at night, conditions of high vagal tone. (Coumel, P., et al. 1978 and 1994). In a landmark study published in 2008, it was demonstrated that vagal induced AF ceased to occur in dogs with surgical removal of the cardiac ganglia surrounding the left atrium, but continued to be induced in dogs with the standard ‘pulmonary vein isolation” procedure (Lemola, K., et al. 2008) currently in

clinical practice. In recent years, therapeutic interventions for AF have now used radiofrequency catheter ablation of selected atrial sites in which high-frequency stimulation induces vagal reflexes. These sites are believed to represent regions of autonomic ganglia of the peripheral nervous system, responsible for the fast synaptic transmission of the parasympathetic effect on the heart. Clinically, targeting of these sites by ablation is believed to offer therapeutic value to reduce AF burden, principally due to destruction of the autonomic ganglia or their peripheral fibres (Scanavacca, M., et al. 2006; Scanavacca, M., et al. 2009; Oh, S., et al. 2011; Lim, P. B., et al. 2011).

The actions of parasympathetic stimulation on cardiomyocytes occur by changing the function of ion channels in response to release of the neurotransmitter acetylcholine and its effects on the activation of the type-2 muscarinic acetylcholine receptor (M2-AChRs). The effects include slowing of pacemaker activity, atrioventricular conduction, and decreased contractile forces. As mentioned above, through the effects on I_{KACH}, shortening of action potential duration also occurs. (Yeh, Y-H., et al. 2007).

1.3.1. Role of acetylcholine- sensitive K^+ current I_{KAch}:

Activation of M2-AChRs by acetylcholine leads to stimulation of the signalling pathway that regulates the acetylcholine- sensitive K^+ current (I_{KAch}). Following M2 binding of Ach, the pathway dissociation of the closely couple G-proteins, Gαi/0 and Gßγ subunits, occurs. The Gßγ subunit is the primary activator of GIRK channels which carry inwardly rectified K+ current (I_{KAch}). This leads to membrane hyperpolarization in SA node and slowing of pacemaker activity (Yamada, M., et al. 1998). The enhanced K current also leads to more rapid repolarization of the cell, shortening APD and effective refractory

period of the myocytes. Further, the M2-AChRs activation lead to inhibition of adenylyl cyclase and decrease cAMP production which lead to decrease I_f current (cAMP-sensitive current) and shift its activation to more negative potential, also slowing pacemaker activity in SA node (Yatani, A., et al. 1990). Decrease of cAMP also leads to decrease in the L-type I_{Ca} current, diminishing the plateau phase of the AP and contribute to shortening of APD duration (Fischmeister, R., et al. 1986). Thus, the cascade effect of Ach binding to the M2-receptor leads to effects on $I_{KAch,}$ I_f current, L-type I_{Ca} current, and cAMP production, which in turn all contribute to the electricophysiologic changes of diminished pascemaker activity and shortened APD, satisfying one of the pre-requisites making the atria susceptible to fibrillation (arrhythmia). The second pre-requisite, conduction velocity slowing, is also due to ACH binding to the M2-receptor, which results in a decrease of gap junction function, impairing cell-to-cell conduction and overall conduction velocity (Yeh, Y-H., et al. 2007).

The multitude of molecular effects due to parasympathetic or vagal activation of the heart are summarized in figure (3). (Yeh, Y-H., et al. 2007; Kwak B. R., et al., 1996).

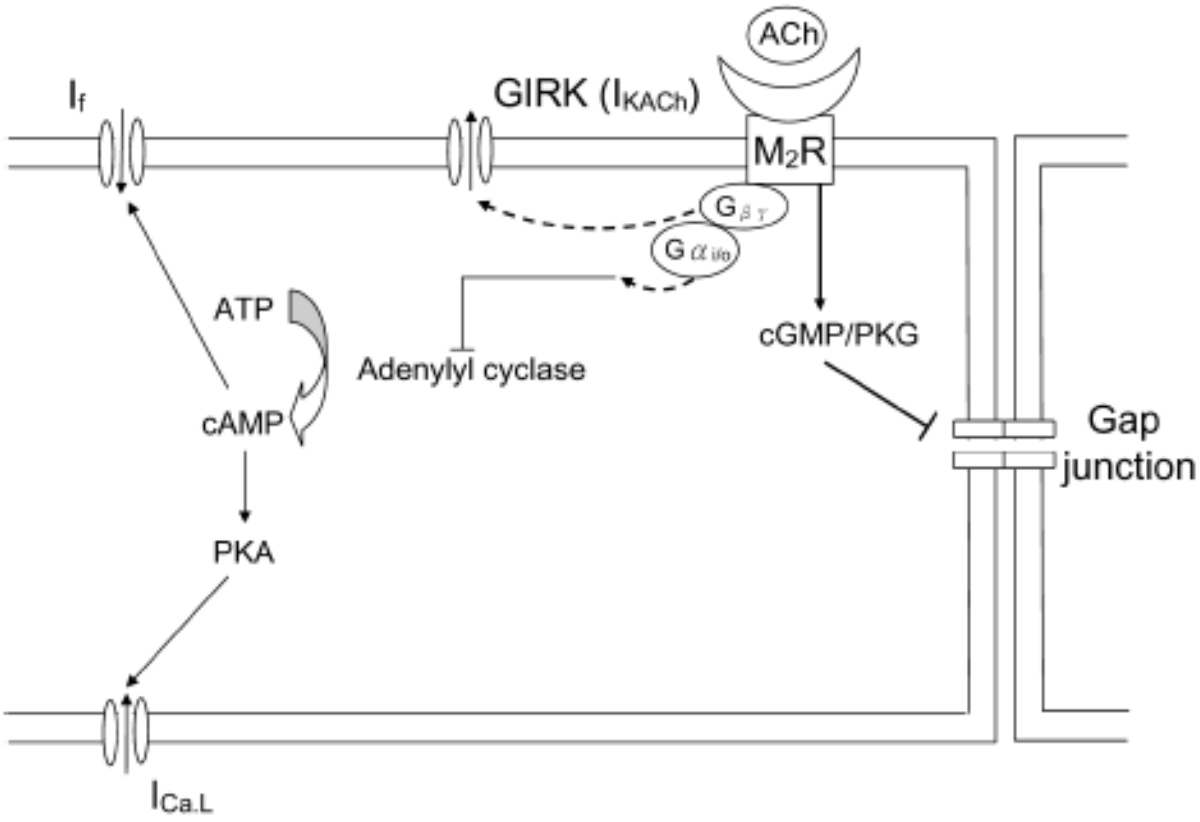

(From Yeh, Y-H., et al. 2007)

Figure 3: Overview of signaling pathways due to activation of M_2AChR. Ach, acetylcholine; M_2, muscarinic acetylcholine receptor subtype 2; GIRK, G-protein regulated inward rectifier k^+ channels; IKACh, acetylcholine- sensitive K^+ current; I_f, pacemaker current; I_{CaL}, L-type Ca^{2+} current; PKA, protein kinase A; PKG, protein kinase G.

Given the electrophysiological effects of Ach (acetylcholine) release on the heart, it is not surprising that many studies demonstrate that AF is induced by Ach perfusion or vagal stimulation, and shows that IKAch is essential in the generation of vagal AF. In a study of the GIRK4 Knockout (IKAch-deficient) mouse model, AF cannot be induced upon Ach infusion (as compared to WT mice), highlighting that the activation of IKAch is required for cholinergic AF (Kovoor, P., et al. 2001). This also suggests that upstream modulators of this current, if altered in their sensitivity to acetylcholine, may play an important role in the pathophysiology of AF.

1.4. Nicotinic acetylcholine receptors (nAChRs)

1.4.1 Definition, Composition, and Location

The ANS is a critical factor in the appropriate regulation of numerous body organs and systems, and complete discussion on this is beyond the scope of this thesis. In the heart, and particularly in the context of AF, the parasympathetic component and its influence on the heart is of critical importance. Acetylcholine (ACH) is the neurotransmitter that is synthesized, stored and released by cholinergic neurons, and the key molecules that transduce the ACH message are the cholinergic muscarinic (mAChRs) and neuronal nicotinic acetylcholine receptors (nAChRs). (Gotti, C., et al. 2004)

Nicotinic acetylcholine receptors (nAchRs) are acetylcholine gated ion channels that belong to the large Cys-loop ligand gated ion channel family which include 5-HT3 receptors, glycine receptor, and GABA receptors. The commonality between all these members in this family is a ‘Cys-loop’ domain found in the N-terminal extracellular

domain, as shown in Figure 4. The nAChRs are a large, diverse, and widely expressed protein family, composed of five subunits encoded from different genes in mammals, and each subunit has four transmembrane domains. nAChRs are widely expressed in the nervous system, where they transduce both adrenergic and cholinergic signals at the synapses in the peripheral ganglia and in various brain areas. (Changeux, J., et al. 2001) The diversity of subunits enables assembly of many heterogeneous pentameric receptors, each with unique biophysical parameters (Treinin, M. 2008).

Functional nAChRs consist of different subtypes, each of which has a specific pharmacology, physiology and anatomical distribution in brain and peripheral ganglia. Since they are activated by a ligand (ACH), they are referred to as ligand-gated ion channels. Early studies characterized nAChRs based on binding assays with nicotinic radio-ligands and focused on nAChRs isolated from regions of the brain, as reviewed in Lukas, R. J., et al. 1992. Based on this method of characterization, there were at least two distinct classes of putative nAChRs defined in the nervous system: one consisting of receptor molecules that bind ^{3}H-agonists with nM affinity but not α-Bungarotoxin (aBgtx), called nAChRs, and the other that bind the agonists with μM affinity and aBgtx with nM affinity called aBgtx-nAChRs. (Lukas, R. J., et al. 1992).

The nAChR subunits that come together in various combinations to form functional nAChRs are encoded by twelve genes, and like all of the other members of the ligand-gated ion channel superfamily, they encode for peptides that all have a relatively hydrophilic extracellular amino terminal portion, followed by three hydrophobic transmembrane domains (M1–M3), a large intracellular loop, and then a fourth hydrophobic transmembrane domain (M4) as shown in next Figure 4b (Hogg R et al., 2003; Gallego, X., et al. 2012). As reported by Le Novere and co workers in 1995, these

subunits have been highly conserved during evolution, have a common ancestor and the same subunit has more than 80% amino acid identity across vertebrate species (Le Novere, N., et al. 1995). The cloned genes are divided into two subfamilies of nine neuronal α subunits (α 2– α 10) and three β subunits (β 2– β 4); each subunit contributes towards the pharmacological specificity of nAChR subtypes (Luetje, C. W., et al. 1991) The nAChR subtypes are also divided into two main classes; homomeric receptors such as (α7, α8, and α9), and heteromeric receptors comprised of α3β 2, α3β4, α4β2, and α4β in an assortment of different compositions. (Lindstrom, J., et al. 2000)

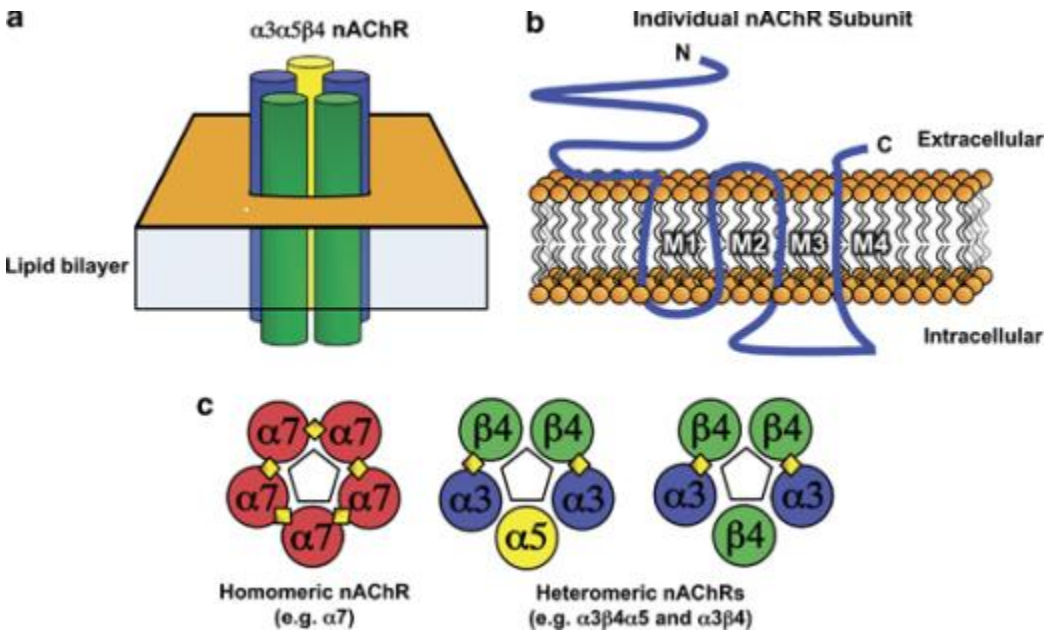

(From Gallego, X., et al. 2012)

Figure 4: Structure of the Nicotinic acetylcholine receptor (nAChR). (a) Schematic representation illustrating the pentameric arrangement of subunits in an assembled nAChR. (b) Conserved domains of a nAChR subunit including the amino (N) and carboxy (C) terminals, transmembrane segments (M1–M4) and the intracellular loop. (c) Assembly of heteromeric and homomeric nAChR subtypes. Individual nAChR subunits are represented as colored circles, with diamonds representing ligand-binding sites. Pentagons in the center of each pentamer represent the pore region.

Many compositions of pentameric nAChR channels are formed in mammals, and two are essential for viability. One of them is the skeletal muscle nAChRs, which are composed of α12ß1δε or α12ß1γδ (not expressed in peripheral ganglia of non-skeletal muscle origin) and are important for the synaptic transmission in the neuromuscular junction (Bibevski, S., et al. 2000). Autonomic ganglia nAChRs are primarily composed of α3, α5, ß2 and ß4 subunits. Alpha 3-containing receptors, co-assembled with α5, β2, and β4 subunits (as α3β2, α3α5β2, α3β4, or α3α5β4), are believed to constitute the basic receptors that respond by Ach-induced fast excitatory postsynaptic transmission in the ANS (Wang, N., et al. 2002; Nelson, M. E., et al. 2001). In addition to these essential nAChR channels there are many receptors that are expressed in the central nervous system of different compositions (Treinin, M. 2008).

The maturation process (assembly and trafficking) of nAChRs starts in the endoplasmic reticulum (ER) where the folding, assembly, and maturation of nAChRs require the Ric-3 protein as a chaperon protein. Post-translational modifications occur at the ER and Golgi apparatus, then the subunits traffic to the surface membrane where they are activated and stabilized, as shown in the Figure 5 (Treinin, M. 2008).

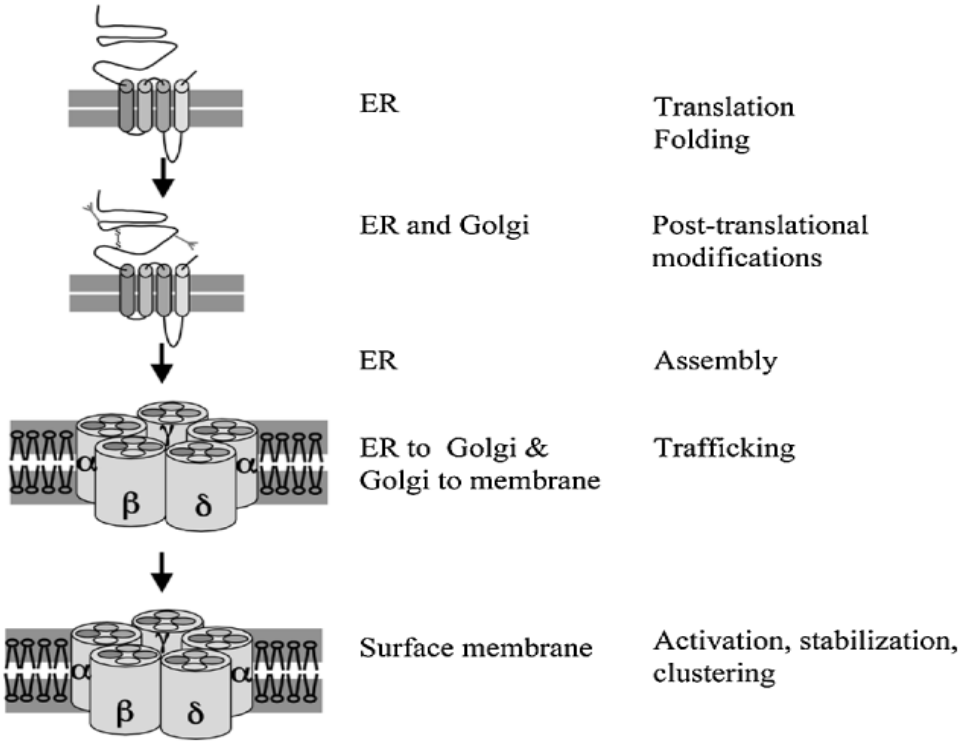

(From Treinin, M. 2008).

Fig 5: A schematic diagram of nAChR organization and maturation. Different steps in the maturation process are presented as occurring sequentially, but in reality folding, post-translational modifications, and assembly are likely to occur in parallel. Above, a schematic representation of a single nAChR subunit before and after post-translational modifications, glycosylation of extracellular residues and disulfide bond formation leading to formation of the Cys-loop. Below, assembled receptor with each subunit depicted as a simple barrel made up of four transmembrane domains and subunit organization indicated according to the mammalian skeletal muscle receptor.

1.4.2 Functional and pharmacological properties of nAChR

It is reported that both α and β subunits determine the functional and pharmacological properties of functional nAChRs; when a β subunit is expressed with any of the α subunits they form channels that vary in their average open times, single channel

conductance, agonist and antagonist sensitivity. (Papke, R. L. 1993) It is also apparent that β subunits regulate the rate at which agonist and antagonist bind and dissociate from the subtypes, and the pharmacological sensitivity of nAChRs. (Papke, R. L. 1993)

In terms of function, nAChRs are ion channels that gate between ion-impermeable closed (C) and ion-permeable open (O) conformations. (Purohit, P., et al. 2007) Acetylcholine binding elicits channel opening through a global conformational transition, The different nAChR subtypes can exist in four different distinct conformations: resting, open, and two desensitized closed channel states (I or D) that are refractory to activation on a timescale of milliseconds (I) or minutes (D); the transition between the different receptor states is regulated by receptor phosphorylation. (Changeux, J. P., at al. 1998). These four conformational states are summarized Figure 6 (Changeux, J. P., et al. 2012).

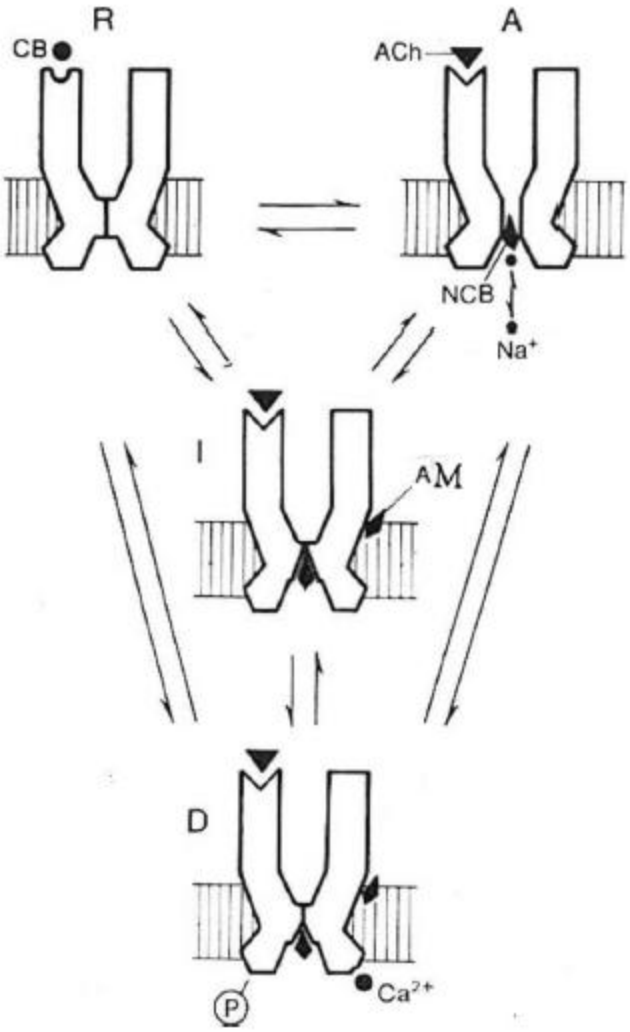

(From Changeux, J. P., et al. 2012)

Figure 6: Minimal four-state model for the allosteric transitions of the nicotinic receptor. CB, competitive (orthosteric) blocker; NCB, noncompetitive (channel) blocker; AM, allosteric modulator; P, phosphorylation site.

1.4.3 nAChR subunits of the peripheral nervous system (ganglia), particularly the ß4 subunit

Expression of ß4 is particularly high in the peripheral nervous system, where ß4-containing nAChRs underlie a significant portion of the Ach induced currents in ganglia (Rust, G., et al. 1994; Xu, W., et al. 1999a,b). β4 subunit is encoded by the *CHRNB4* gene, located on chromosome 15q25.1. The gene length is 17.48 kb, the mRNA coding region 2972 bp and is translated into 498 amino acid. (Albuquerque, E. X., et al 2009). The α3ß4 nAChR functional pentamer, with or without α5, is the most abundant functional receptor, particularly in the peripheral nervous system (Chavez-Noriega, L. E., et al. 1997).

Recent studies of mice with genetic ablation of single or double nicotinic subunits (knock out) or a single gene mutation (knock in), have shed light on the role of nAChRs and their major physiological functions. In mice, knock out of the α3 subunit is lethal. Mice are unable to live more than one week due to multiorgan dysfunction and failure (Champtiaux, N., et al. 2002; Xu, W., et al. 1999a). Similar phenotypes were also reported in the double β2-β4 knock-out mice. (Xu, W., et al. 1999b).

However, most relevant to cardiac electrical function, only the β4 knock-out mouse is viable and a demonstrates a cardiac phenotype, showing an attenuated bradycardic response to high-frequency vagal stimulation (Wang, N., et al. 2003). In addition, these mice showed a largely reduced nicotinic agonist-induce contractile response in ilea (Wang, N., et al. 2003). These results strongly support the hypothesis that the presence of β4 subunits are required and a vital component for cholinergic signalling to the heart and

gut, and that the presence of β4 is essential for complete vagal-mediated parasympathetic signalling to these end-organs. On the other hand, α5 knockout mice study showed supersensitivity to hexamethonium C6 blockade and significantly increase ileal contractile responses to the nicotinic agonists cytosine and epibatidine, but not dimethylphenylpiperazinium iodine (DMPP) and nicotine (Wang, N., et al. 2002), suggesting that the addition of α5 subunits to nAChR stoichiometry has a slight opposing effect to B4 subunits.

Knowledge of the importance of parasympathetic and vagal tone in inducing AF in humans, and the vital role of the β4-nAChR subunit in transmitting cholinergic signalling to the heart, as gleaned from mouse studies, led us to the basis of our first hypothesis in this thesis. Namely, that rare, genetic variants in the B4 gene, *CHRNB4,* may be identified in otherwise healthy patients with AF and that these variants may show functional changes consistent with a gain-of-function in response to ligand stimulation.

1.5 Resistant to inhibitors of cholinesterase: The Ric-3 Protein

The transmembrane protein Ric-3 (Resistant to inhibitors of cholinesterase) functions as a molecular chaperone of nAChRs. It is required for the maturation of nAChRs by playing an important role in their folding, assembly, surface expression, and functional properties (Millar, N. S. 2008). Lansdell and coworkers provide evidence for the mechanism of Ric-3 and its role in nAChRs maturation by interaction of Ric-3 with unassembled receptor subunits within the endoplasmic reticulum and the facilitation of the their folding and assembly of receptor subunits (Lansdell, S. J., et al. 2005).

Ric-3 is composed of two transmembrane domains followed by coiled-coil domain, both N and C- terminii are located in the cytoplasm, and the region between the two transmembrane regions is a proline-rich domain that seems to have a critical role in Ric-3's chaperone activity as shown in Figure 7. Ric-3 is highly expressed in the heart, skeletal muscle, and brain. It is located within the endoplasmic reticulum, with no evidence for localization in the cell surface (Millar, N. S. 2008).

First studied in *xenopus* oocytes, Ric-3 co-expression was shown to enhance α7-nAChR whole-cell current amplitude. This effect was associated with enhanced surface expression of α7 receptor. Using immunoprecipitation analysis to study the association between Ric-3 and α7 cell surface expression in mammalian HEK293 cells, Williams and colleagues showed that co-expresion of Ric-3 was essential for cell surface expression of α7. Cells without Ric-3 co-expression did not show cell surface α7 (Williams, M. E., et al. 2005). Surprisingly and paradoxically, Ric-3 was noted to inhibit the whole cell current amplitude produced by two other human nAChRs α4β2 and α3β4 as well as a mouse 5-HT3 serotonin receptor. However in mammalian cells, co-expression of hRic-3 resulted in significantly enhanced surface expression as well as the functional expression of α3β2, α3β4, α4β2, and α4β4 hetromeric nAChRs (Lansdell, S. J., et al. 2005). This paradoxical effect in oocytes and mammalian cell lines may be due to absence of some additional required proteins in oocytes. As well, alternative splicing of Ric-3 may also explain this difference in its effects, as analysis of human Ric-3 transcripts identified multiple isoforms resulting from alternative splicing and alternative promoters (Treinin, M. 2008).

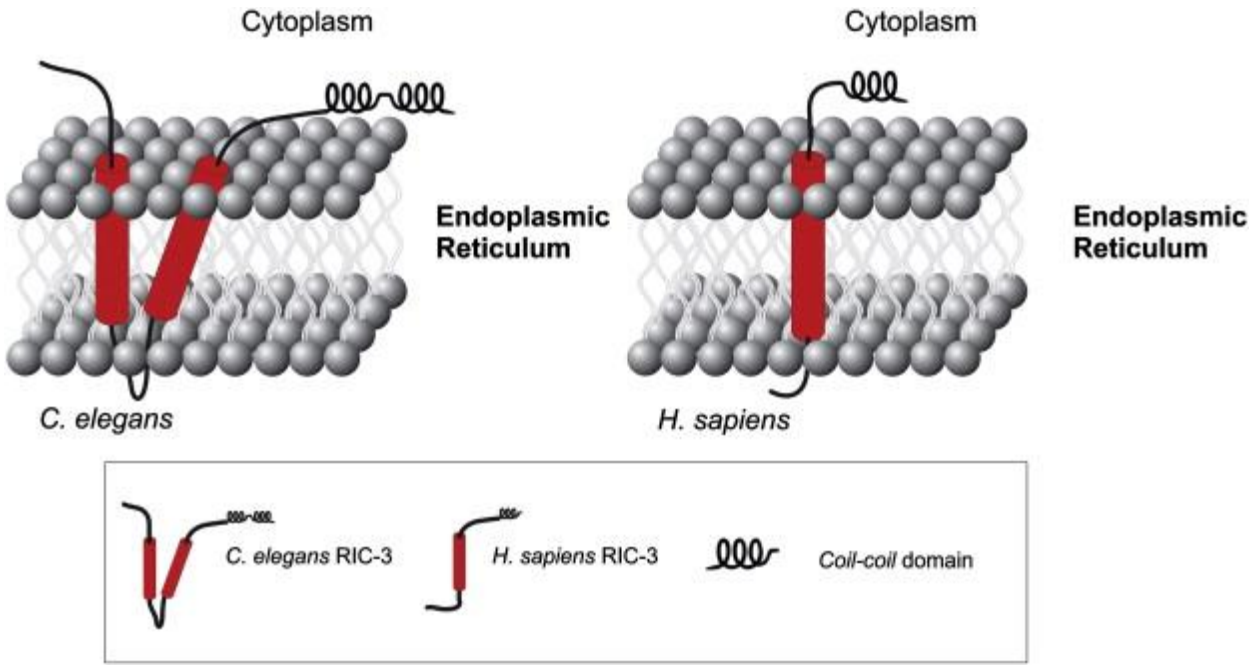

(From Vallés, A. S., et al. 2012)

Figure 7: The RIC-3 protein. In C. *elegans*, the RIC-3 protein (left) comprises an N-terminal domain (the exact position of which has not yet been clearly established), a membrane-spanning domain separated by a proline-rich spacer, and a C-terminal domain exposed to the cytoplasmic compartment, which possesses two coiled-coil domains. The suggested topology of the H. sapiens RIC-3 homolog (right) differs structurally simply in having a shorter N-terminal domain and only one coiled-coil domain.

The concept that Ric-3 promotes nAChRs assembly intermediates within ER to influence their maturation into functional receptors is also supported by the following evidence from several studies. Firstly, physical interaction of Ric-3 with nAChR subunits is observed in the ER when Ric-3 is co-expressed with mutant nAChR subunits that are unable to exit the ER (Halevi, S., et al. 2002). Secondly, localization studies of Ric-3 fail

to observe it at the surface membrane but rather only within the ER compartment (Halevi, S., et al. 2002; Castillo, M., et al. 2005). Lastly, Ric-3 interacts with unassembled subunits suggesting the importantance of Ric-3 in stabilization and in enabling trafficking of functional receptors (Lansdell, S. J., et al. 2005; Ben-Ami, H. C., et al. 2005).

Wang and colleagues propose a membrane topology model of mouse RIC-3 (mRIC-3) protein using the simplicity of the α7 system and Ric-3's role in nAChR assembly. They report that mRIC-3 is a type I protein with a single transmembrane segment that is localized to the ER by a cleavable signal sequence. They also suggest a mechanism of how RIC-3 facilitates folding of α7 subunits and their assembly into mature receptors, shown in Figure 8 (Wang, Y., et al. 2009). They propose the coiled-coiled domains of RIC-3 leads to heterodimer formation, and that this heterodimer formation may then bring the α7 monomers into close apposition and facilitate their oligomerization. The α7 /mRIC-3 complex is free to associate with another α7 monomer bound to mRIC-3 and this process continues until the formation of a complete functional nAChR pentamer (Wang, Y., et al. 2009).

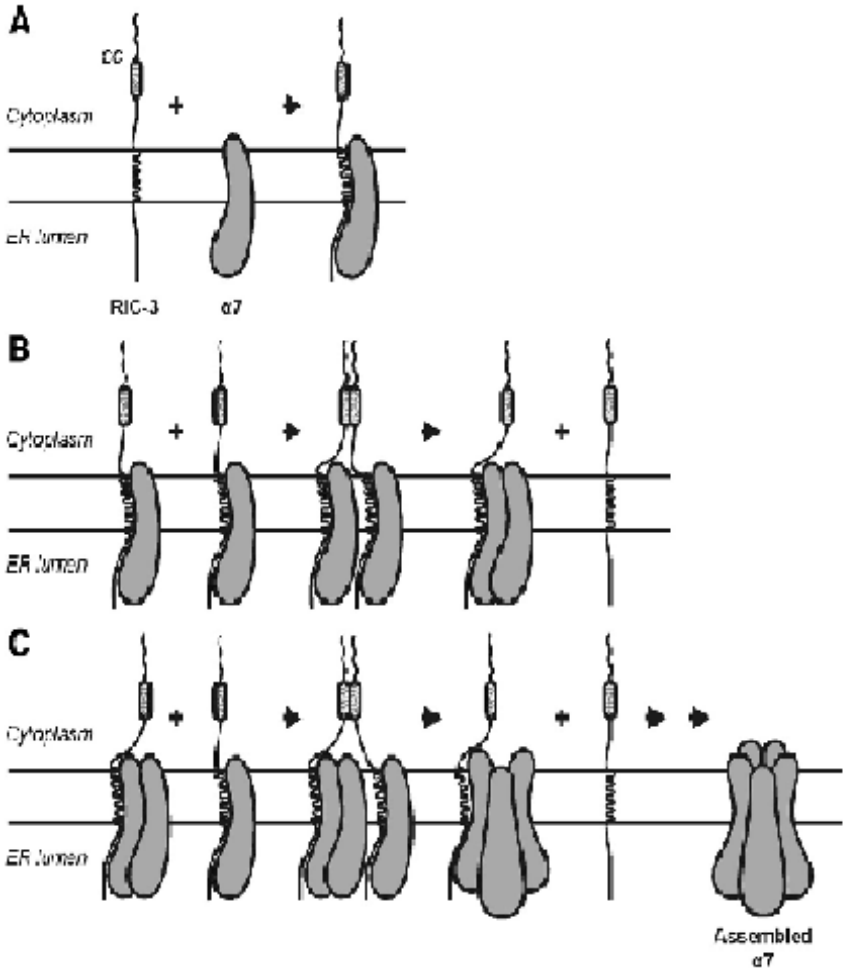

(From Wang, Y., et al. 2009)

Figure 8: Model for the facilitation of α7 assembly by mRIC-3. A, mRIC-3 binds to the α7 monomer via interactions that do not involve the coiled-coil domain (CC). B, The self-association of mRIC-3 mediated by the coiled-coil domain brings the α7 monomer/ mRIC-3 complexes into close proximity and facilitates the dimerization of α7 monomers. Upon formation of the α7 dimer, one of the two RIC-3s is released. C, The α7 dimer/mRIC-3 complex is then free to associate with another α7 monomer bound to mRIC-3. Iteration of this process results in the formation of a complete pentamer. In principle, this scheme is generally applicable to the mechanism of RIC-3 facilitation of both homopolymeric and heteropolymeric receptor assembly.

Ric-3 can promote or inhibit cell surface delivery of nAChRs depending on its expression level.

The discussion till now has emphasized the chaperoning effect of Ric-3 and its role in promoting cell surface expression and hence increased function of nAChRs. However, it has now been established, at least in *in vitro* systems, that the level of Ric-3 expression, low or high, may have opposing effects on promoting nAChR surface expression. This is relevant to effects on Ric-3 that may be caused by genetic mutations in the protein.

The studies of Alexander and colleagues have shed light on the effect of low or high Ric-3 expression levels. They studied the effects of varying expression levels of Ric-3 on the cell surface expression of the Bugarotoxin receptor (BgtR), a nAChR analog, and on the α7-nAChR subunit. They demonstrated that at low levels of Ric-3, the surface delivery, BgtR assembly, and endoplasmic reticulum release was promoted. At high levels of Ric-3 expression, the surface delivery of BgtR was suppressed, but not its assembly and the BgtR was observed to be retained in the ER by Ric-3- containing aggregation. (Alexander, J. K., et al. 2010). This can explain the dual effect of Ric-3 that had been shown in different studies. It was also indicated that in PC12 cells, a neural cell, endogenous Ric-3 expression levels are low and appear to promote α7 subunits assembly and surface delivery. Their results indicate that at higher Ric-3 levels, longer- lived interactions subunits predominated that retained BgtRs in the ER, and as similarly shown in neurons, Ric-3 retained α7subunits in the ER subcompartment of dendrites. At low levels short-lived interaction with α7 subunits predominated and Ric-3 facilitated BgtRs assembly, ER release, and cell-surface delivery. (Alexander, J. K., et al. 2010).

Further complexity to the regulation of Ric-3 function was proposed by Shteingauz and co-workers. They reported that another protein (BATH-42) targets Ric-3 to degradation via CUL-3 mediated ubiquitylation (Shteingauz, A., et al. 2009). They also demonstrated the important of the regulation of Ric-3 levels and its subsequent effect on nAChR surface expression, consistence with what was reported by Alexander and co-workers. Anna and colleagues propose that Bath-42 degradation of Ric-3 is a mechanism that protects cells from the deleterious effects of excess Ric-3. They also propose that the conserved coiled coil domain of Ric-3 is likely responsible for the interaction between Ric-3 and BATH-42.

Summary

In summary, the ANS exerts parasympathetic influence on the heart by fast synaptic transmission via peripheral ganglia located adjacent to the heart. The molecular mediators of this cholinergic signalling are the nAChRs, which upon binding of ACH at their synaptic clefts leads to rapid release of ACH onto cardiac myocytes, imparting changes in cardiac electrophysiology hastened by muscarinic receptors present on the myocytes. Indirectly, the ability of nAChRs to transmit this signalling is influenced by the endogenous co-expression of Ric-3, which promotes nAChR function. This physiology forms the basis of the hypotheses of this research, whereby genetic alterations in key molecular mediators of this process may alter ligand-mediated function, and potentially promote vulnerability to AF by creating a 'hypersenstive' parasympathetic pathway. Our research has focused the *Ric-3* and *CHRNB4* genes, and the characterization of rare mutations identified in these genes.

1.6 RATIONALE, HYPOTHESES, OBJECTIVES

1.6.1 Rationale

The autonomic nervous system has been recognized as a critical component in arrhythmogenesis, particularly AF. Recognition that AF has a heritable component has led to an intensive search for the genetic culprits responsible for the disorder. The identification of genes that predispose to the arrhythmia has begun to provide further insight into the factors that govern its initiation and maintenance. Improved insight into the pathophysiology of the condition guided by a sophisticated understanding of the genetic underpinnings, promises to lead to more innovative treatment strategies that will ameliorate the care of affected patients.

As summarized in the previous section, our study focuses on genes encoding key molecular mediators of cholinergic signalling in the heart, the *CHRNB4* gene, that encodes the β4 subunit of nACHR channels, and the *Ric-3* gene, encoding for the Ric-3 protein which functions as a molecular chaperone of nAChRs. The main mediators of fast synaptic transmission in cardiac ganglia are predominantly the α3β4 subtype. A deeper understanding of the influence of molecular mediators of cholinergic signalling may provide novel insight and/or molecular targets in AF.

1.6.2 General hypotheses: Rare genetic variants in the *CHRNB4* and *Ric-3* genes will be identified in patients with AF, and functional characterization will indicate altered, possibly enhanced, nAChR function. Such findings will suggest that gene variations in molecular mediators of cholinergic signalling may contribute to AF vulnerability in some patients.

2.6.3 Objectives:

1- **To explore the potential genetic role of *CHRNB4,* a mediator of cholinergic signalling to the heart, in human patients with AF.**

   A. To perform comprehensive genetic screening of the *CHRNB4* gene in AF patients.

   B. To assess the functional effects of novel or rare mutations of the *CHRNB4* gene identified in humans with AF.

2- **To explore the potential genetic role of the *RIC-3* gene, a modulator of nAchR function, in human patients with AF.**

   A. To perform comprehensive genetic screening of the *Ric-3* gene in AF patients.

   B. To assess the surface and functional expression of nAChRs on mammalian cells transfected with identified mutated Ric-3, as compared to WT-Ric-3.

Chapter 2

2.1. nAChRs: Material and Methods

2.1.1. β4 nAChR (*CHRNB4*) subunit- Study subjects:

Blood samples for lymphocyte DNA analysis were collected from 315 AF patients. This cohort represented patients with presumed 'lone AF'. Patients with secondary causes of AF, including severe, uncontrolled hypertension, moderate-severe valvular disease, cardiomyopathy or late-onset AF (age >65 yrs) were excluded from enrollment. Control DNA samples (n=600) were kindly provided from the laboratory of Dr. Ruth McPherson. These samples were originally collected as controls for the Ottawa Heart coronary artery disease project and represented an elderly cohort (age > 70 yrs) with no reported cardiovascular disease history. These patients were also questioned about their medication usage. Blood samples for the purpose of DNA analysis were collected with written informed consent and were approved for study by the institutional review board of the University of Ottawa Heart Institute.

2.1.2. Mutation Detection in β4 nAChR subunit:

Genetics analysis was performed on genomic DNA isolated from the blood samples collected from both AF patients and Controls. The entire coding sequence of *CHRNB4* gene was directly sequenced using standard Sanger sequencing methods. Mutation detection was performed by analysis of the sequence electropheragrams of each of the six coding regions of *CHRNB4* gene, Oligonucleotide primers for the coding regions of each exon were designed using the known cDNA and genomic sequence as shows in Table 1.

The PCR was performed under the following conditions: 50ng of genomic DNA was subjected to 35 cycles of amplification in a volume of 25µl containing 1µM of each forward and reverse primer, 200mM of DNTP, 1.5mM Mg^{2+}, 0.2 U of Taq polymerase.

The PCR amplification conditions were as following; One cycle at 95^{o}C for one minute as a denaturation step, followed by 35 cycle at 94 ^{o}C for 45s, 56 ^{o}C for 45s and 72 ^{o}C for 1 minute, followed by one cycle at 72 ^{o}C for 7 minute as the final elongation step.

Table 1: Oligonucleotide primers sequences for the coding regions of each exon of *CHRNB4* gene, showing the exon number, forward primer (F), Reverse primer (R):

F1- 5'CCCTGTGACCCCACAGCGGAGCT3' R1- 5'AGTCCAGCCCCTTTCAGCCCAACC3'
F2- 5'TCTCAGCTCTCCCTGCTGCCACAGG3' R2- 5'ATGAGCGGCCTCTCCACCTGAGCC3'
F3- 5'ATCCATTTGTGAGGCTCCTCCTTCC3' R3- 5'TTGCAGGTCCACTGCCACCAAAGG3'
F4- 5'GGCAGTGGACCTGCAAGTGACAGG3' R4- 5'AGCAGAGATGGGGCTCAGGGTTGG3'
F5a- 5'CCAAAGGGCTCTTCAGTGAGTTCTG3' R5a- 5'TGGCAGGTAGAAGACGAGGATGGC3' F5b- 5'AGCCTCTGTTCTACACCATCAACCTC3' R5b- 5'GCTTGGTCACGCATGACTTGCTGG3' F5c- 5'CTTCCTGCACAAGCTGCCTACC3' R5c- 5'CTATCTGAGCCCTTTCTGTTGGG3'
F6- 5'CCAGAGAGTAAGGGCCTGACTCG3' R6- 5'GAAAGAAGCAGCAAAGTGCCCACC3'

2.1.3. Cell Culture HEK tsa-201 cell line:

Functional expression studies were performed in a HEK tsa-201 cell line, a cell line that does not express nAChR subunits. To maintain these cell lines, we used growth media containing DMEM, 2mM L- Glutamine, 10% FBS, and 1% Pen/Strep antibiotics. Cultures were maintained at 37 ^{o}C and 5% $CO_{2.}$

2.1.4. HEK tsa-201 cell transfection:

A glass coverslip was placed at the bottom of each of a 24-well plate before plating the cells and these coverslips were coated with ploy-L-lysine 0.1 mg/ml. Cells were transiently transfected with CHRNA3 and CHRNB4 plasmids (ORIGENE, Rockville, MD) in OPTI-MEM medium (Invitrogen, Carlsbad, CA) using lipofectamine 2000 (Invitrogen, Carlsbad, CA). A total amount of 1µg of each plasmid per well and 500ng of YFP fluorescent protein plasmid were used to select cells for patching, Preliminary testing has indicated that 1 µg of alpha3 and 1 µg B4 cDNA is adequate for eliciting nAChR current post-transfection. For heterozygote studies of B4 mutants, 0.5 ug of wt and 0.5 ug of mutant cDNA were transfected with 1 ug alpha3 cDNA. The plasmid and liofectamine were mixed with 50µl of OPTI-MEM medium and incubated for 15 min at room temperature and then mixed together followed by 15 min incubation at room temperature then the complexes were added to the cells with 500µl of the media. For Calcium Imaging Technique, 35 mm dishes with glass bottom were using for transfection.

2.1.5. Cloning and site-Directed Mutagenesis of β4 nAChR subunit:

We have obtained our cDNA clones for the alpha3 nAChR subunit and B4 nAChR subunit through purchase from ORIGENETM (Rockville, MD). The cDNA clone was sequenced before using to ensure normal sequence. Five as forward primers (F) and one as reverse primer (R);

F1-5'TTCCCTGGTCCTTTTCTTCCTGGTCG3'

F2- 5'GATCCCTGCAAAGCGCATCTGGTTGC3'

F3- 5'GAGAAGGACAGTGAACCCACAAGACC3'

F4- 5'CACCAGCGTCTGTGTGCTCAATGTGC3'

F5-5'ATTTCTGGCTGCGGTCCTCTGGGAGG3'

R1- 5'CCAGACATTGGTGGTCATGATCTGC3'

We used the site directed mutagenesis kit (Stratagene^{TM}, La Jolla, CA) to generate the specific rare genetic variants identified in AF patients. Primers for each variant as shown in table 2.

Table 2: Oligonucleotide primers sequences designed for site directed mutagenesis to create the variants that were detected in the *CHRNB4* gene, showing the name of variant, forward primer (F), Reverse primer (R):

S417P-F 5'GATTTCTGGCTGCGGTCCCCTGGGAGGTTCCGACAGG3'
S417P-R 5'CCTGTCGGAACCTCCCAGGGGACCGCAGCCAGAAATC3'
R349C-F 5'CCTTCCTCTTCATGAAGTGCCCTGGCCCCGACAGC3'
R349C-R 5'GCTGTCGGGGCCAGGGCACTTCATGAAGAGGAAGG3'
A273T- F 5'GTGCATCTCAGTGCTGCTGACACTGACATTCTTCCTGCTG3'
A273T- R 5'CAGCAGGAAGAATGTCAGTGTCAGCAGCACTGAGATGCAC3'
R39C- F 5'ACGACCTTCTGAACAAAACCTGTTACAATAACCTGATCCGC3'
R39C- R 5'GCGGATCAGGTTATTGTAACAGGTTTTGTTCAGAAGGTCGT
S198G- F 5'GCATGGATGACTTTACTCCCGGTGGTGAGTGGGACATAGTGG3'
S198G- R 5'CCACTATGTCCCACTCACCACCGGGAGTAAAGTCATCCATGC3'

2.1.6. Functional and physiological study of mutant β4 nAChR subunit:

The functional effect of wild type and mutant *CHRNB4* on nAChR function was performed by calcium imaging and whole cell patch clamp techniques.

2.1.6.1. Whole-cell patch clamp recording:

Patch clamp recordings were conducted 36–48 h after transfection, The whole-cell currents were recorded with use of Axopatch 200A integrating patch-clamp amplifier and

clampex 9 data acquisition software (both from Molecular devices, USA), as described by Nelson, M. E., et al. 2001). The composition of the buffer in the recording electrode was 140 mM Gluconic Acid, 140 mM CsO_4, 10 mM EGTA, and 10 mM HEPES, adjusted to pH 7.2 with CsO_4. The composition of extracellular path buffer was 140 mM NaCl, 5mM KCl, 2 mM $CaCl_2$, 1 mM $MgCl_2$, 5 mM HEPES, and 5 mM D-glucose, adjusted to pH 7.3 with 1N NaOH. Recording electrodes were pulled from borosilicate glass capillaries (Sutter, USA) on PIP5 two stage vertical pipette puller (NARISHIGE, JAPAN) and electrode resistance was typically 2-4MΩ. The series resistance was typically 3-5MΩ. All measurements were performed at room temperature (22-24 ^{o}C) and a membrane potential of -60mV. ACH (10μM) and NIC (1mM) dissolved in the extracellular buffer was applied using cell-flow technique.

For EC50 and current density recordings, currents were elicited by applying the ligand (ACH or NIC) for 1–2 s to wild type, mutant, or simulated heterozygous receptors with an SF- 77B Perfusion Fast-Step system (Warner Instruments, USA). To assess for receptor desensitization, repetitive doses of nicotine were applied at 90 second intervals.

Data was analyzed offline by use of pClamp8 and Origin6 (Microcal) software. Dose-response curves to nicotine and acetylcholine were plotted using average peak currents obtained at the indicated ligand concentrations and normalized to the current obtained in the presence of 100 mM agonist. All averaged data were plotted as a mean +/- standard error of the mean. Statistical analysis comparing values for wt and mutant clones were performed using one-way analysis of variance, where $p < 0.05$ is considered as significant.

2.1.6.2 Calcium Imaging Techniques:

Calcium Imaging were performed 36-48 h after the transfection by loading the cell with 5µM Ca green1/am dye (life technology, Carlsbad, CA) for 70 min. the calcium signal was recorded by Monochrome CCD Camera (Cohu Inc, Poway, CA). The photos were analyzed and measured using Axon Imaging Workbench program (AIW2.2). The recording was started before, during, and after applying 20µM of ACH or 5µM of NIC. Cells were always loaded with path solution contain 140 mM NaCl, 5mM KCl, 2 mM CaCl2, 1 mM MgCl2, 5 mM HEPES. pH adjusted to 7.4 using 1N of NaOH.

Assay Solution containing Ca green1/am dye was prepared by dissolving 1µL of Dye in 400 µL of regular solution followed by incubation in Ultrasound Cleaner for 7 Min to dissolve the DMSO. The Nicotine and acetylcholine were prepared on the same day of experiments by dissolving appropriate volumes in regular bath solution.

2.2 Ric-3: Material and Methods

2.2.1. Ric-3 Study subjects:

Blood samples for lymphocyte DNA analysis were collected from 315 AF patients and 600 controls, as described above. Blood samples were collected with written informed consent and were approved for study by the institutional review board of the University of Ottawa Heart Institute.

2.2.2. Mutation Detection in the *Ric-3* gene:

Genetics analysis was performed on genomic DNA isolated from the blood samples collected from both AF patients and Controls. The entire coding sequence of the *Ric-3* gene was directly sequenced. Mutation detection was performed by analysis of

sequencing electropheragrams of the six coding regions of Ric-3; Oligonucleotide primers for the coding regions of each exon were designed using the known cDNA and genomic sequence as shown in Table 3.

The PCR was performed under the following conditions: 50ng of genomic DNA was subjected to 35 cycles of amplification in a volume of 25µl containing: 1µM of each forward and reverse primer, 200mM of DNTP, 1.5mM Mg2+, and 0.2 U of Taq polymerase. The PCR amplification conditions were as following: one cycle at 95 ^{o}C for one minute followed by 35 cycle at 94 ^{o}C for 45s, 56 ^{o}C for 45s in testing exon 1,4,5 and 58 ^{o}C in testing exon 2,3 and 6, 72 ^{o}C for 1 minute, followed by one cycle at 72 ^{o}C for 7 minute as final elongation.

Table 3: Oligonucleotide primers sequence for the coding regions of each exon of Ric-3, showing the exon number, forward primer (F), Reverse primer (R):

F1	5'gacagtggaggtgaagatgcgtgc3'
R1	5'caagcagcgttctccgtactcttcg3'
F2	5'ggcctcttttataccttaatgatttggtg3'
R2	5'ctatcctaagtacctcatgaagaggaggc3'
F2	5'catgatagccatctttaaaatagtagaagag3'
R2	5'gaggaggcaggatttaaagagatg3'
F3	5'ccgtgactgaggttctgagctgc3'
R3	5'acccacagactgtccctgtggct3'
F3	5'ctgagctgctgttgatgtgctatacctcc3'
R3	5'ctctgcctccattttgctctctgctacc3'
F4	5'caggtttagggagttgtctctgatgg3'
R4	5'gccactgcacccagcctgaatttatt3'
F5	5'ccagacagaccatagtgatgtttacgtcc3'
R5	5'ccaggggcaggagaagggcattagct3'
F6	5'ggataggatggctgctgcctgag3'
R6	5'ggagagagaggtcaccttgggac3'

2.2.3. Cell Culture of HEK cells stably expressing the nAChR subunits alpha3, alpha5 and beta4; Constructs and Antibodies:

Functional expression studies were performed in HEK cells stably expressing the nAChR subunits alpha3, alpha5 and beta4, a kind gift from Dr. Jon Lindstrom from the University of Pennsylvania. To maintain this cell lines we used growth media containing DMEM, 2mM L- Glutamine, 10% FBS, 1% Pen/Strep antibiotics, 0.25 mg/ml Zeocin, 0.3 mg/ml G-418, and 0.1 mg/ml Hygromucin. Cultures were maintained at 37 ^{o}C and 5% $CO_{2.}$

Full-length Ric-3 cDNA clone in pCMV6-XL5 victor was purchased from ORIGENE^{TM}, Rockville, MD. This was subcloned into pECFP-N1 vector, as follows: fusion of cyan fluorescent protein (CFP) to the C terminus of Ric-3 was generated by subcloning Ric-3 into pECFP-N1 vector (BD Biosciences, Toronto, Canada). An EcoRI site was inserted just 5' to the start codon of Ric-3 using the Quikchange site-directed mutagenesis Kit (Qiagen, Venlo, Netherlands). An Age I site was inserted just 3' to the stop codon which was also changed to amino acid using the Quikchange site-directed mutagenesis Kit (Qiagen, Venlo, Netherlands) the site-directed mutagenesis was performed using forward primer 5'CCGGTTCCGGCTGAATTCTGCACCTGCGACCACCGTG3' and reverse primer 5'CAGACTGGCACCGGTCCCTCTAAACCCTGGGGGTTACGC3' . Double digestions by EcoRI and AgeI for the pECFP victor and the PCR product, then the products were separated on agarose gel to confirm specific amplification of the band of interest and purified using gel purification. Ligation of the PCR product and the vector was performed at 6°C overnight with the DNA Ligation Kit (Stratagene, La Jolla, CA) using a ratio of Insert:Vector of 3:1. Ligated products were transformed into subcloning efficiency DH5a competent Cells (Invitrogen, Carlsbad, CA) following the company

protocol. Transformed bacteria were plated on agar plates with kanamycin antibiotic. Colonies were picked and grown overnight in LB broth with kanamycin antibiotic and a miniprep was performed the following day. DNA isolated from the minipreps was Sanger sequenced to confirm an errorless coding sequence and to assure the *Ric-3* gene was in frame with the start codon of the florescent protein, in addition to assure the variants genetic code. Bacteria containing the sequence-confirmed clones were grown in large scale overnight in LB broth with kanamycin and purified next day using a maxiprep.

Antibodies

1. Mouse monoclonal antibody raised against cyan fluorescent protein (CFP). (Biosensis, Thebarton, Australia)
2. Rabbit polyclonal antibody raised against nACHR α3 subunit. (Santa Cruz Biotechnology, Santa Cruz, CA
3. Monoclonal antibody raised against TFR as a Western blot control.(Santa Cruz Biotechnology, Santa Cruz, CA)

2.2.4. Cell transfection of HEK cells stably expressing the nAChR subunits alpha3, alpha5 and beta4:

A glass coverslip was placed at the bottom of each of a 24-well plate before plating the cells and these coverslips were coated with ploy-L-lysine 0.1 mg/ml. HEK293 stably expressed α3α5β4 nAChRs were transiently transfected with Ric-3 plasmid in OPTI-MEM medium using lipofectamine 2000 (Invitrogen, Carlsbad, CA). A total amount of 100ng Ric-3 plasmid per well and 100ng of YFP fluorescent protein plasmid were used for transfection. Preliminary testing has indicated that 100ng Ric-3 cDNA is adequate for

eliciting nAChR current post-transfection. The plasmid and liofectamine were mixed with 50µl of OPTI-MEM medium and incubated for 15 min at room temperature and then mixed together followed by 15 min incubation at room temperature; the complexes were then added to the cells with 500µl of the media. For Calcium Imaging Technique, 35 mm dishs with glass bottom were using for transfection. For patch clamping technique, cell transfection were performed using GeneJuice Transfection Reagent (EMD Millipore Corporation, Temecula, CA). Cells were plated on 35 mm dishes, A total amount of 500ng Ric-3 plasmid per well and 500ng of YFP fluorescent protein plasmid were used for transfection. Three µl of GeneJuice Transfection Reagent were mixed with 100µl of OPTI-MEM medium (Invitrogen, Carlsbad, CA) then vortexed and incubated for 5 min at room temperature. Ric-3 plasmid and YFP plasmid were then added, followed by 15 min incubation at room temperature then the complexes were added to GeneJuice Transfection Reagent and OPTI-MEM medium complex and incubated for an additional 15 min. then The complexes were then added to the cells. The day after, transfected cells were plated again and distributed on a 24- well plate with glass coverslips coated by ploy-L-lysine 0.1 mg/ml. Cells were tested 36-48 hours after transfection.

2.2.5. Cloning and site-Directed Mutagenesis Ric-3 construct:

Ric3 cDNA clone in the pCMV6-XL5 vector was purchased from the ORIGENETM, Rockville, MD. We have sequenced this clone using three forward primers and one reverse to confirm appropriate sequence.

F1-5’CTCCACAGTGCAGAGAGTCGCT3’;

F2- 5’CCAGTTTTGAGCTTGCTCAACTG3’;

F3- 5’CGAGGATCCTGCTGTCTTGGCAG3’;

R1- 5’CTGCCCCATCAGACCTCTTCCA3’.

Two common, minor allele SNPs were detected in the clone: C130Y and D351N. To generate a wild type clone we performed a site directed mutagenesis to reverse these SNPs, as all variants in AF patients were detected without these two SNPs, using primers 5’CAGAGGATGGGAAATGCTATACTGCCATGCC3’ as forward primer and 5’GGCATGGCAGTATAGCATTTCCCATCCTCTG3’ as a reverse primer normal C130Y and 5’GTTGGGCATCAGCACAGATAAAGCATATACAGG3’ as a forward primer and 5’CCTGTATATGCTTTATCTGTGCTGATGCCCAAC3’ as a reverse primer for normal D351N. The exception was AF case harbouring the rare S294L Ric-3 variant, whom along with his screened relatives were detected to carry C130Y and D351N in addition to S294L variant. Two primers were designed for each variant and the site directed mutagenesis kit (Stratagene, La Jolla, CA) were used to generate the variant cDNA. The untagged Ric-3 cDNA was used for the patching clamping and calcium imaging experiments.

2.2.6. Functional and physiological study of nAChRs on cells transfected with wild-type or mutant Ric-3:

We performed these studies in HEK cells stably expressing the nAChR subunits alpha3, alpha5 and beta-4, a kind gift from Dr. Jon Lindstrom from the University of Pennsylvania.

Functional effects of wild type and mutant Ric-3 on nAChR function were performed by whole cell patch clamp techniques, calcium imaging, radioligand binding assay, immunoblotting, and localization studies using the confocal microscope.

2.2.6.1. Whole-cell patch clamp recording:

The whole-cell currents were recorded 36-48 hours after transfection with use of Axopatch 200A integrating patch-clamp amplifier and clampex 9 data acquisition software (both from Molecular devices, USA), as described by Nelson, M. E., et al. 2001). The composition of the buffer in the recording electrode was 140 mM Gluconic Acid, 140 mM CsO_4, 10 mM EGTA, and 10 mM HEPES, adjusted to pH 7.2 with CsO_4. The composition of extracellular path buffer was 140 mM NaCl, 5mM KCl, 2 mM $CaCl_2$, 1 mM $MgCl_2$, 5 mM HEPES, and 5 mM Dglucose, adjust to pH 7.3 with 1N NaOH. Recording electrodes were pulled from borosilicate glass capillaries (Sutter, USA) on PIP5 two stage vertical pipette puller (NARISHIGE, JAPAN) and electrode resistance was typically 2-4MΩ. The series resistance was typically 3-5MΩ. All measurements were performed at room temperature (22-24 ^{o}C) and a membrane potential of -60mV. ACH (10µM) and NIC (1mM) dissolved in the extracellular buffer which was applied using cell-flow technique.

2.2.6.2. Calcium Imaging Technique:

Calcium Imaging was performed 36-48 hours after transfection, by loading the cell with 5µM Ca green1/am dye (life technology, Carlsbad, CA) for 70 min. The calcium signal was recorded by Monochrome CCD Camera (Cohu Inc, Poway, CA). The photos were analyzed and measured using Axon Imaging Workbench program (AIW2.2). The

recording was started before, during, and after applying 20µM of ACH or 5µM of NIC. Cell were treated with path solution containing 140 mM NaCl, 5mM KCl, 2 mM CaCl2, 1 mM MgCl2, 5 mM HEPES. pH adjusted to 7.3 using 1N NaOH.

2.2.6.3. [3H]- Epibatidine Radioligand Binding Assay:

Radioligand Binding assays were performed 36-48 hours after transfection; HEK293 stably expressed α3α5β4 nAChRs transiently transfected with Ric-3 plasmid was removed from the growth media and 500µl of blocking solution were added and the cells were incubated at room temp for 30 Min. Pre-cooled culture plates were used (containing cells on ice in 4ºC cold room for 15 to 20 min) to insure that no radioligand will enter the cells. All the reagent, media, and washing buffers were also cooled down. In the meantime, both hot and cold assay media was prepared. Hot assay buffer contained DMEM Optimum, 0.2% BSA, and 35 nM [3H]- Epibatidine (PerkinElmer ,Waltham, MA). Cold assay buffer for nonspecific binding contained DMEM Optimum, 0.2% BSA, 35 nM [3H]- Epibatidine, 2mM of Nicotine, and 2mM of Carbacol. Blocking solution was removed and each well was incubated with 100µl of assay buffer for 30 Min at 4ºC. Assay buffer solution was removed, cells were washed X3 rapidly, followed by 1X 5 min incubation and 2 more rapid washes using 1X PBS. Cells were removed from ice and dissolved by incubation with 500 µl of 0.1 NaOH for 1 hour. Finally, 300 µl were removed for counting using a gamma counter. An aliquot of 200 µl was used for protein assay using the Markwell Lower assay. To perform the Markwell Lower assay, Reagents A, B, and C were prepared (reagent A containing 10g Na2CO3, 2g NaOH, 0.8g NaK Tartrate, and 5g SDS/500ml, reagent B containing 4g CuSO4-5H2O/100ml, and reagent

C was prepared by 1:1 dilution of Folin Ciocalteu Reagent: H2O). 100 parts reagent A were combined with 1 part reagent B to made AB mix. A standard curve was prepared using 0-5µg BSA from 1mg/ml stock. (0, 2.5, 5, 10, 25, 50µg). Samples were prepared using 50 µl from NaOH lysates neutralized with HCL. 1.0ml of the reagent AB was mixed to blank, standards, and samples. Those samples were vortexed and incubated a minimum of 10 minutes at room temperature. 100 µl of reagent C (1:1 dilution of Folin Ciocalteu Reagent: H2O.) was added to all tubes and vortexed, then incubated for 45 min at room temperature. 200 µl from each tube was transferred to a 96 well plate. Absorbance was read at 655nm on plate reader.

2.2.6.5. Immunoblotting:

Western blotting were performed 36-48 hours after transfection to measure the level of α3 subunits as a key indicator to surface expression of nAChRs on HEK 293 stably transfected cell with α3, β4, and α5 and transient transfected with Ric-3 WT or mutant clones. Membrane extracts were bound with specific anti-rabbit anti-α3 subunits (Santa Cruz Biotechnology, Santa Cruz, CA) or anti-mouse, anti-CFP antibody (Biosensis, Thebarton, Australia) as tagged Ric-3 protein fused with CFP fluorescence protein was used in this experiment. For loading control we bound the membranes with anti-mouse, anti-TFR (transferrin receptor) antibody (Abcam, Cambridge MA). Prior to the experiments, 700,000 cells were plated in each 100 mm tissue culture dish for each variant in growth media. Two days later, 1 hour before the transfection reagent was added, the growth media was changed to DMEM only, without FBS or antibiotic. Cells were transfected

with 11 ug Ric-3 cDNA per plate using Lipofectamine 2000 (Invitrogen, Carlsbad, CA) as per the manufactory protocol. Media was changed and 10ml of growth media was added after 5 hours of transfection. Cell harvesting was performed 36 hours after transfection by scrape in PBS, and centrifuging with 1100 rpm for 10 min. Pellets was washed 1X with PBS. Cell membrane fraction was prepared by resuspending pellets in 1 ml sorbitol microsome buffer (50 mm Hepes-KOH, pH 7.2, 250 mm sorbitol, 10 mm KCl, 1.5 mm MgCl2), incubating for 20 min on ice, and then disruption with 30 passages through a 23G needle; the membranes were isolated by centrifuging with 55,000 rpm for 30 min at 4^{o}C and membrane pellets were re-suspended in 250 ul in TX100 buffer/ pH6 (40 mM Tris-maleate, pH 6.0, 100 mM NaCl, 2 mM CaCl2, 1 mM MgCl2, 1% TX-100). A 25G needle was used to homogenize the pellet, and tubes were then incubated on ice for 15 Min. The homogenenates were centrifuged at 21,000 x g for 20 min and supernatants were transferred to new tubes. Protein concentrations were determined using Bradford Protein Assay Gels run in the cold room at 40 mA for 2-3 hours. Transferring was done overnight with a cold circulating bath - 100 mA (transfer buffer + 20% methanol) (Almontashiri, N. A., et al. 2013).

3. Results

3.1. Rare Mutations were detected in *CHRNB4* gene.

3.1.1. Genetic screening of CHRNB4 gene:

We screened the CHRNB4 gene in 315 AF cases and 600 individuals recruited as healthy controls. Specifically, at the time of recruitment the control population reported no history of arrhythmias. We observed an excess of rare variants (mean allele frequency < 0.02) in cases vs controls. This occurred for the *CHRNB4* gene (5/330 cases vs 1/600 controls, p=0.02 Fishers exact test). In 4 of 5 patients, nocturnal AF as a common trigger of the arrhythmia was present, consistent with a vagal-induced onset. The 5 rare variants noted in cases are denoted as: R39C, S198G, T273A, and S417P, and one patient we detected a double mutant (T343A, R349C) as shown in Figure 9. The R349C variant is not a rare variant and is known to present in 1.2% of Caucasians according to public databases. The other noted variants affect highly conserved amino acid residues within the gene.

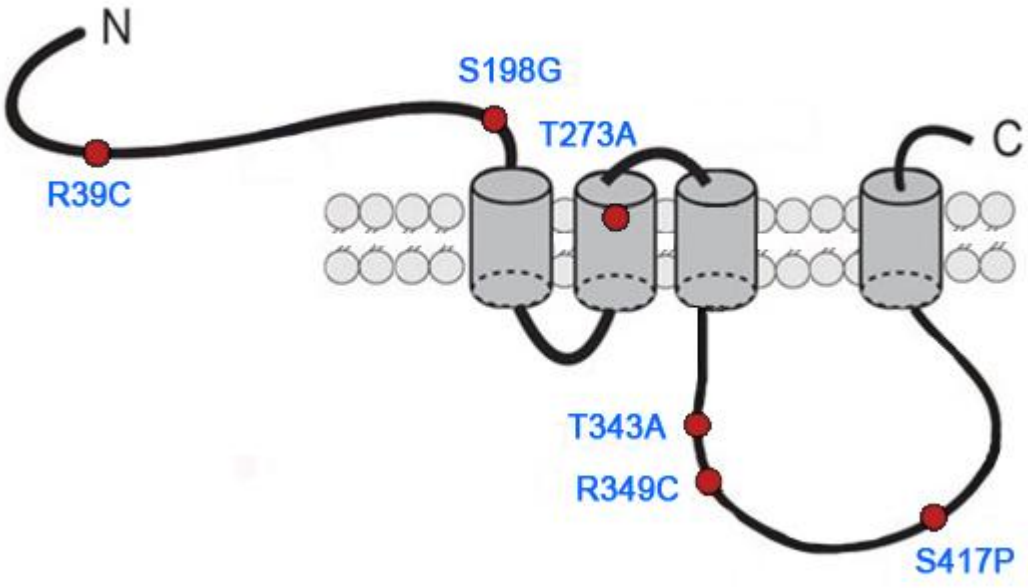

Figure 9: **A schematic diagram of β4 subunit of nAChR**; Conserved domains of a nAChR subunit including the amino (N) and carboxy (C) terminals, transmembrane segments (M1–M4) and the intracellular loop. R39C and S198G mutations located on the extracellular domain, T273A mutation located on the second transmembrane, T343A, R349C, and S417P mutations located on the intracellular loop.

3.1.2. Effect of mutant β4 subunits on the physiological properties of alpha3-Beta 4-nAChRs.

3.1.2.1. Electrophysiological studies in mammalian HEK tsa-201 cells

Functional study of these variants was performed using HEK tsa201 cells known to be naive for endogenous expression of nAChR subunits. This cell line was tested pre-transfection to confirm no detectable nAChR current in the presence of ACH ligand. In contrast, cells co-transfected with α3 and β4 nAChRs subunits evoked a significant current responding to 1 mM of ACH as shown in Figure 10.

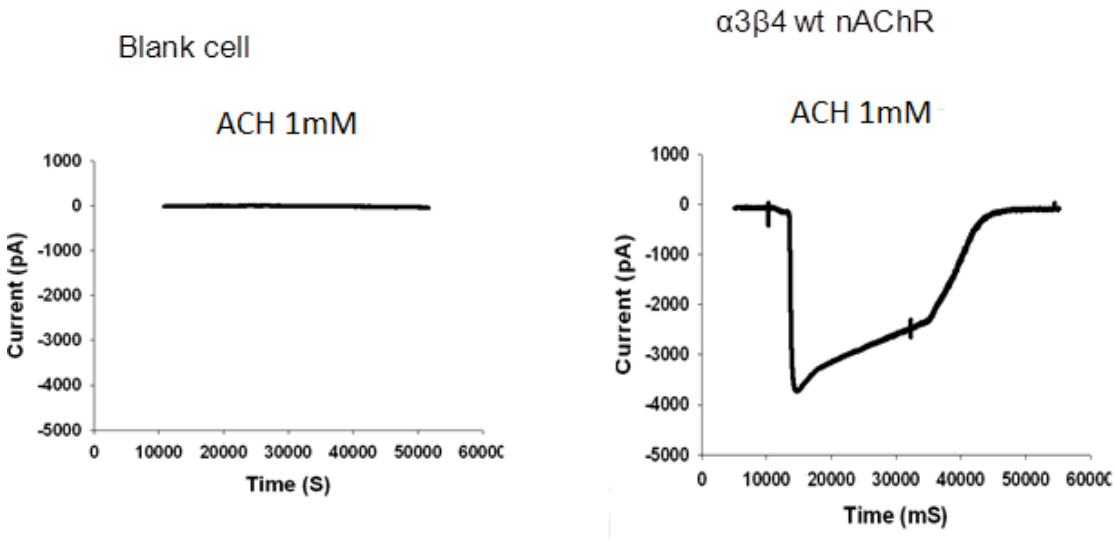

Figure 10: Representative traces of currents elicited upon application of 1 mM of ACH from HEK cell tsa-201 cell non transfected (left), versus transfected with 1µg α3Wt and 1µg WT β4 (right). Significant differences, determined by two-tailed student's t test, are indicated (*, P< 0.05).

3.1.2.2. Homozygous Mutant β4 subunits cause a significant difference in cell current density evoked by 1 mM NIC compared to WT.

Recording the cell current evoked by 1 mM NIC show a significant increase in recorded current in cells transfected with S417P or S198G compared with WT. In contrast, a significant decrease in current was recorded in the cells transfected with A273T

compared to WT, while no significant difference in currents were detected in cells transfected with R39C or the double mutant (T343A, R349C) compared to Wt. These results are shown in Figure 11.

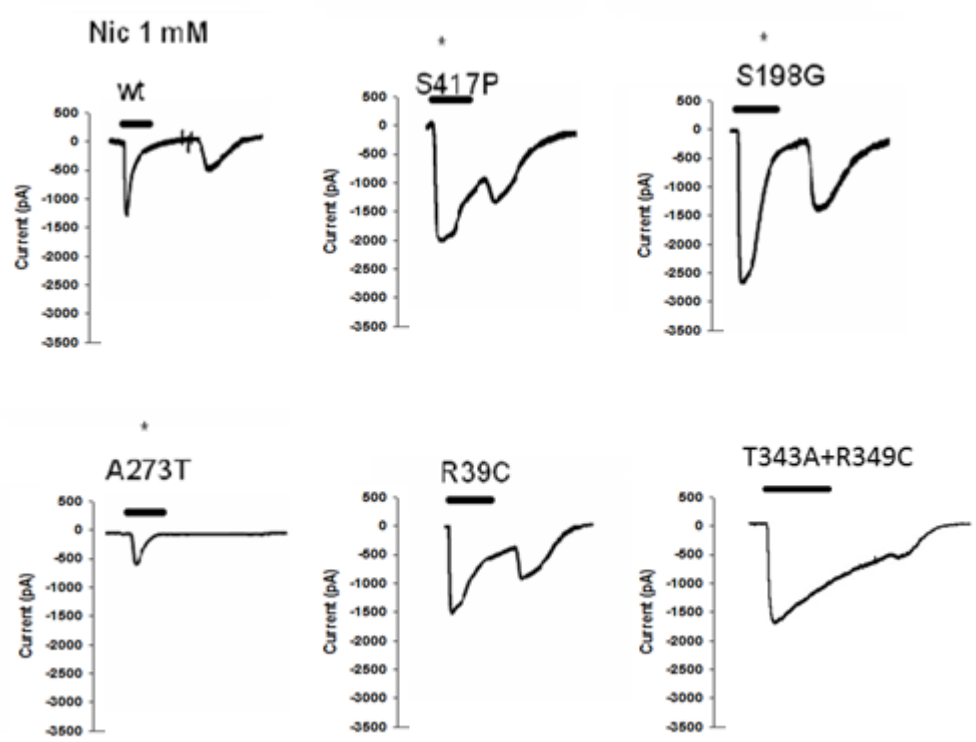

Figure 11: Representative traces of currents elicited upon application of 1 mM of Nic from HEK cell tsa-201 cell transfected with 1µg α3Wt and 1µg WT β4 (WT nAChRs), 1µg α3 WT and 1µg mutant β4 (Mutant nAChRs). Significant differences, determined by two-tailed student's t test, are indicated (*, $P < 0.05$).

3.1.2.3. Homozygous Mutant β4 subunits cause a significant difference in cell current density evoked by 1 mM ACH compared to WT.

Recording the cell currents in response to 1 mM ACH showed a significant increase in cells transfected with S417P or S198G compared to those transfected with WT, a

significant current decrease was recorded in cells transfected with A273T compared to WT, while no difference were detected in cell currents recorded in cells transfected with R39C or the double mutant (T343A, R349C) compared to Wt. These results mirror the results seen with nicotine as ligand, as described above. Results are demonstrated in Figure 12.

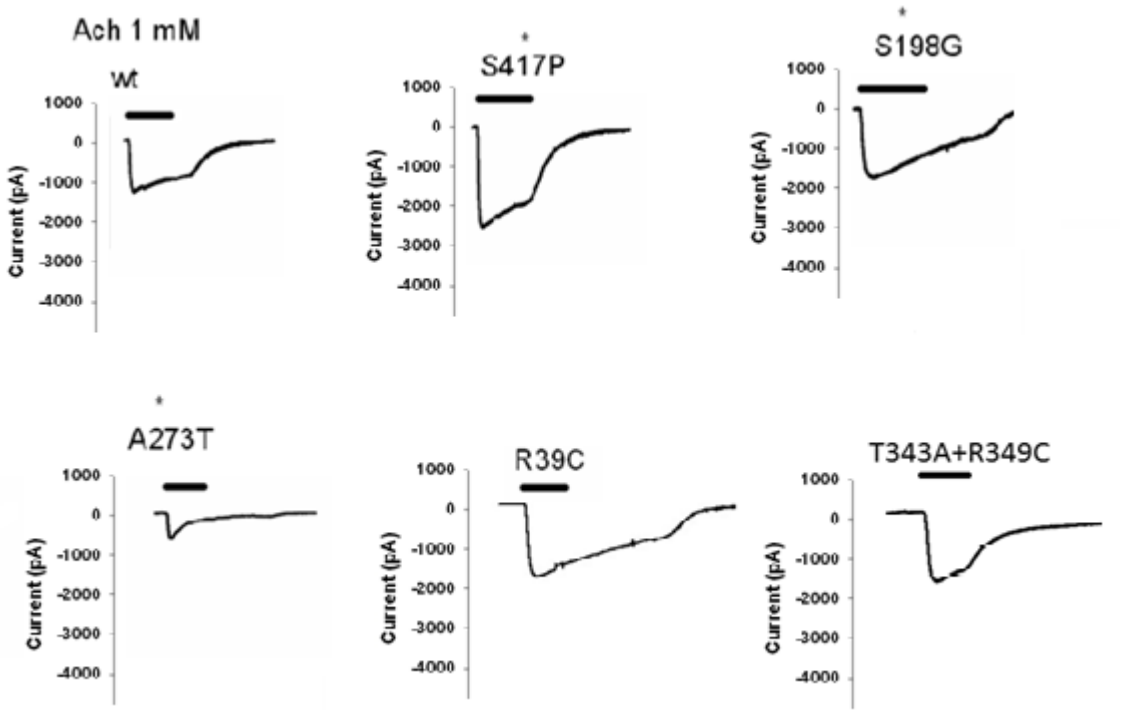

Figure 12: Representative traces of currents elicited upon application of 1 mM of ACH from HEK cell tsa-201 cell transfected with 1µg α3Wt and 1µg WT β4 (WT nAChRs), 1µg α3Wt and1µg mutant β4 (Mutant nAChRs). Significant differences, determined by two-tailed student's t test, are indicated (*, P< 0.05).

3.1.2.4. Heterozygous S417P or S198G Mutant β4 subunits significantly increase current evoked by 1 mM ACH compared to WT.

Since patients have the observed rare mutations in the heterozygous state, experiments were repeated for those mutations showing an increased current density to assess the effect in the heterozygous state. Cell currents were recorded on cell transfected with heterozygous construct (both WT and S417P) or (WT and S198G). The result showed that both heterozygous states significantly enhance cell current compared to those cells transfected with WT only, as shown in Figure 13.

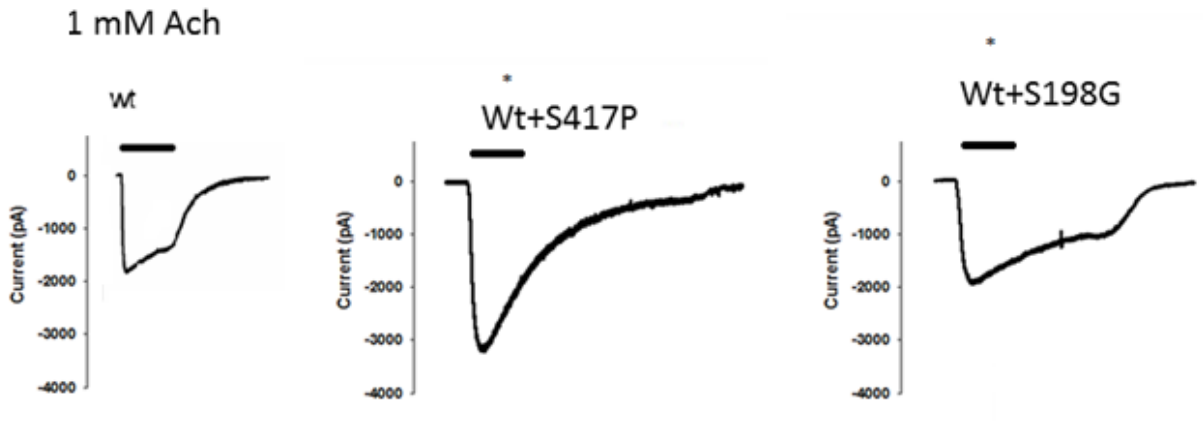

Figure 13: Representative traces of currents elicited upon application of 1 mM of ACH from HEK cell tsa-201 cell transfected with 1µg α3Wt and 1µg WT β4 (WT nAChRs), 1µg α3Wt and 0.5 µg β4 WT and 0.5 µg mutant β4 (Mutant heterozygous nAChRs). Significant differences, determined by two-tailed student's t test, are indicated (*, P< 0.05).

Among the five rare variants that were detected in AF patients but not in controls, S417P or S198G both homo and heterozygous states significantly enhance cell current density evoked by NIC or ACH ligands. Figure 14 summarizes the normalized currents of the patch clamp experiments.

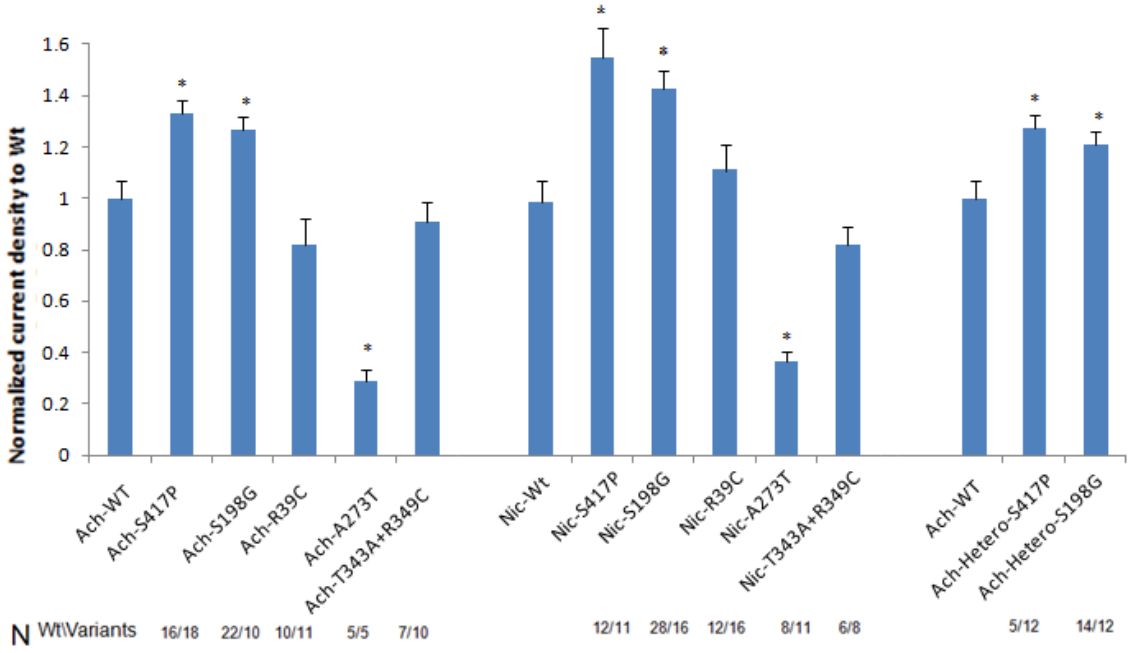

Figure 14: Effect of β4 subunit variants on tsa-201 Cells transfected with 1µg of WT α3 and 1µg WT β4 or1µg mutant β4 plasmid on current density. Normalized current densities for cells elicited upon application of 1mM ACH and 1mM NIC, N = WT\Variants ACH-S417 (n=16/18), ACH-S198 (n=22/10), ACH-A273T (n=10/11), ACH- R39C (n=5/5), ACH-(T343A, R349C) (n=7/10), ACH-Hetero S417P (n=5/12), ACH-Hetero S198G (n=14/12). NIC-S417 (n=12/11), NIC-S198 (n=28/16), NIC-A273T (n=12/16), NIC- R39C (n=8/11), ACH-(T343A, R349C) (n=6/8). Significant differences, determined by two-tailed student's t test, are indicated (*, P< 0.05)

EC50 Dose-response curves

We studied the dose-response relationships in tsa-201 cells transfected with 1µg of WT α3 and 1µg WT β4 or 1µg mutant β4 plasmid in response to ACH. Mutant S417P showed significant increase in receptor sensitivity compared to WT, as shown by left shift as in Figure 15 A, while A273T showed a significant decrease in receptor sensitivity compared to WT, as shown by a right shift in Figure 15 A. Others variants showed no difference in sensitivity compared to WT. We also studied the dose-response relationships for tsa-201

cells transfected with 1µg of WT α3 and 1µg WT β4 or 1µg mutant β4 plasmid in response to NIC. The results showed no difference in receptor sensitivity in response to NIC compared with WT as shown in Figure 15 B.

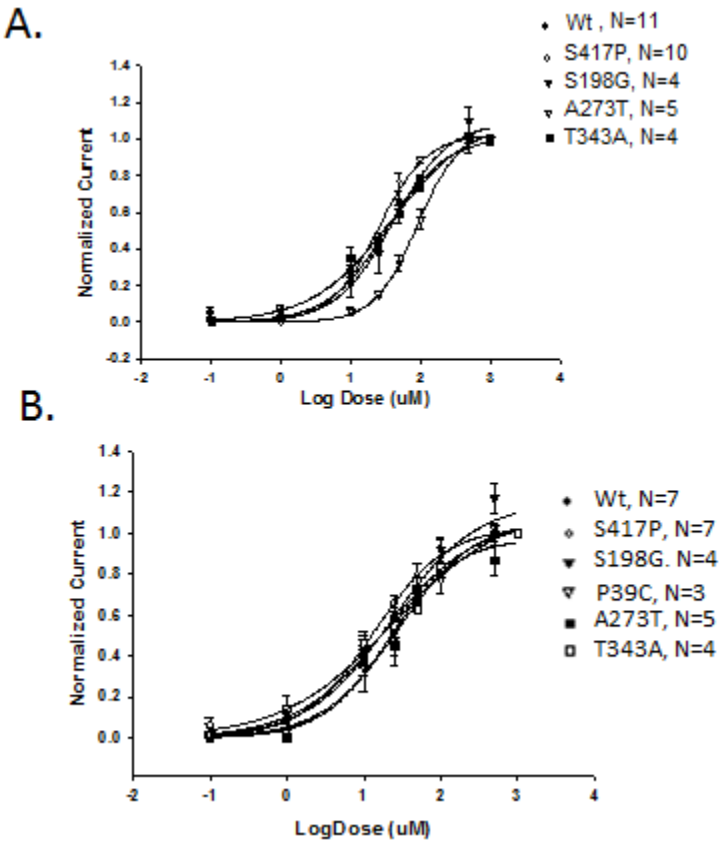

Figure 15: The dose-response relationships nAChRs on HEK tsa-201 Cells transfected with 1µg of WT α3 and 1µg WT β4 or1µg mutant β4 plasmid in response to ACH (A) and NIC (B). The currents are plotted as a function of the logarithmic scale of the ACH concentration (A) and NIC concentration (B). Values are normalized to the maximal current evoked by the highest ACH or NIC concentration. Curves through the data were created as the best fit to the Hill equation. Error bars indicate the standard error of the mean.

3.1.2.5. nAChR desensitization with mutant versus wt CHRNB4

We studied the desensitization and time course of recovery of the nAChRs for the five variant homozygous and heterozygous states, as compared to WT. Four of 5 mutants showed a significant delay in desensitization time (S417P, S198G, R39C, and A273T) as shown in Figures 16-20, respectively. This delay in receptor desensitization predicts a more sustained current following repetitive ligand stimulation, and translates into a gain-of-function for the receptor.

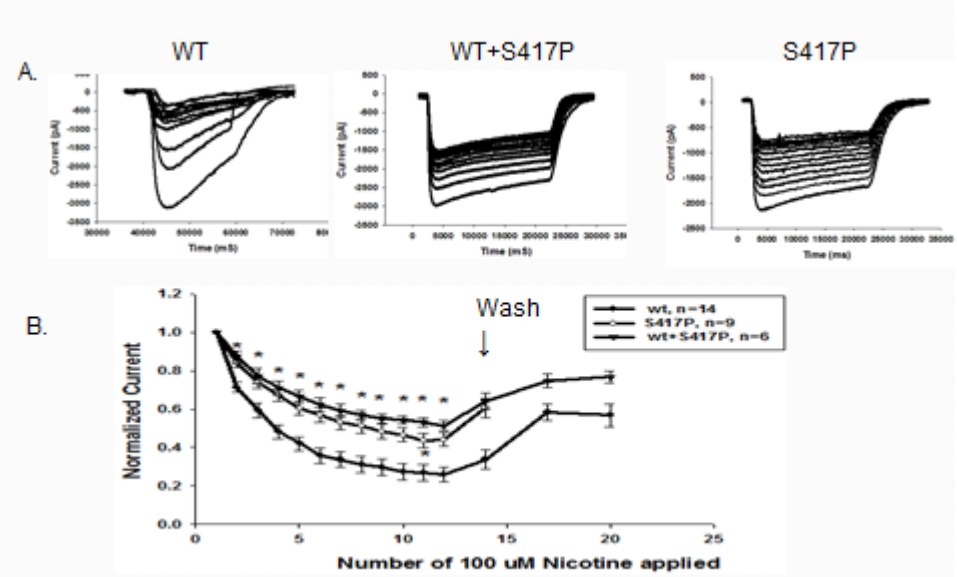

Figure 16: The desensitization of α3β4 wt, wt plus S417P (heterozygous) and S417P (homozygous) in tsa-201 Cells. A, the representative traces of currents elicited upon application of 100μM NIC each 90 sec up to 12 time from HEK for α3β4 wt, S417P (heterozygous) and S417P (homozygous). B, The time course of desensitization of α3β4 wt (closed circle), wt plus S417P (heterozygous)(closed triangle) and S417P (homozygous)(open circle). Significant differences, determined by two-tailed student's t test, are indicated (*, P< 0.05).

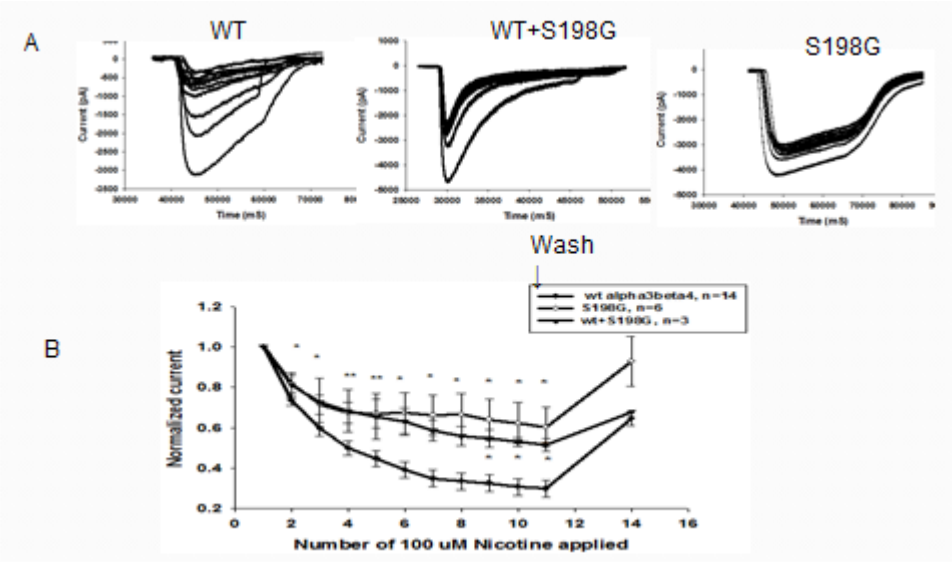

Figure 17: The desensitization of α3β4 wt, wt plus S198G (heterozygous) and S198G (homozygous) in tsa-201 Cells. A, the representative traces of currents elicited upon application of 100μM NIC each 90 sec up to 12 time from HEK for α3β4 wt, S198G (heterozygous) and S198G (homozygous). B, The time course of desensitization of α3β4 wt (closed circle), wt plus S198G (heterozygous)(closed triangle) and S198G (homozygous)(open circle). Significant differences, determined by two-tailed student's t test, are indicated (*, P< 0.05).

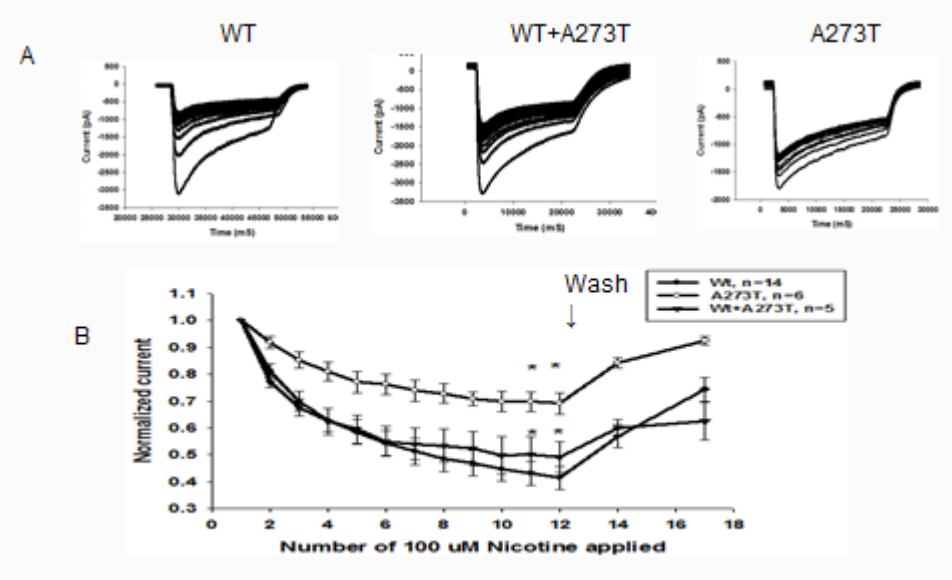

Figure 18: The desensitization of α3β4 wt, wt plus A273T (heterozygous) and A273T (homozygous) in tsa-201 Cells. A, the representative traces of currents elicited upon application of 100μM NIC each 90 sec up to 12 time from HEK for α3β4 wt, A273T (heterozygous) and A273T (homozygous). B, The times course of desensitization of α3β4 wt (closed circle), wt plus A273T (heterozygous)(closed triangle) and A273T (homozygous)(open circle). Significant differences, determined by two-tailed student's t test, are indicated (*, P< 0.05).

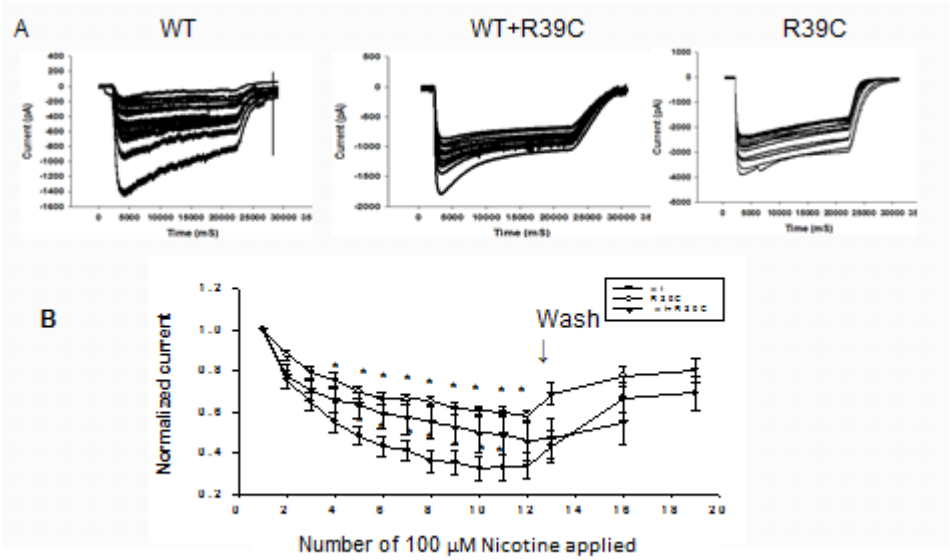

Figure 19: The desensitization of α3β4 wt, wt plus R39C (heterozygous) and R39C (homozygous) in tsa-201 Cells. A, the representative traces of currents elicited upon application of 100μM NIC each 90 sec up to 12 time from HEK for α3β4 wt, R39C (heterozygous) and R39C (homozygous). B, The time course of desensitization of α3β4 wt (closed circle), wt plus R39C (heterozygous)(closed triangle) and R39C (homozygous)(open circle). Significant differences, determined by two-tailed student's t test, are indicated (*, P< 0.05).

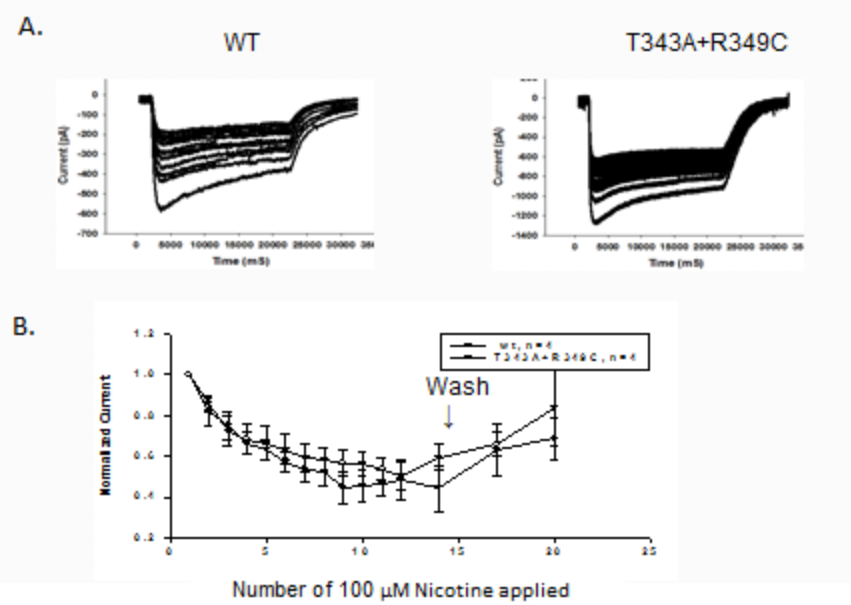

Figure 20: The desensitization of α3β4 wt, T343A plus R349C (heterozygous) in tsa-201 Cells. A, the representative traces of currents elicited upon application of 100µM NIC each 90 sec up to 12 time from HEK for α3β4 wt, T343A plus R349C (heterozygous)). B, The time course of desensitization of α3β4 wt (closed circle), wt T343A plus R349C (heterozygous)(closed circle). Significant differences, determined by two-tailed student's t test, are indicated (*, P< 0.05).

3.1.2.6. Calcium Imaging

In correlation with patch clamp experiments, results show an increase in calcium signal response to 20µM of both NIC and ACH in cells transfected with S417P, S198G, or R39C, while A273T shown a significant decrease compared to WT as shown in figure 21.

Summary of Results

Four of 5 rare variants demonstrated altered function in response to ligand. A unifying observation of these 4 variants was a delay in desensitization, indicating a gain-of-function effect. Delayed desensitization predicts a more sustained current response to repetitive ligand exposure, as might be expected occur in setting of increased neural activity or parasympathetic stimulation. This physiologic response observed in these rare variants may predict a 'hypersensitivity' response of 'vagal' stimuli in these selected patients.

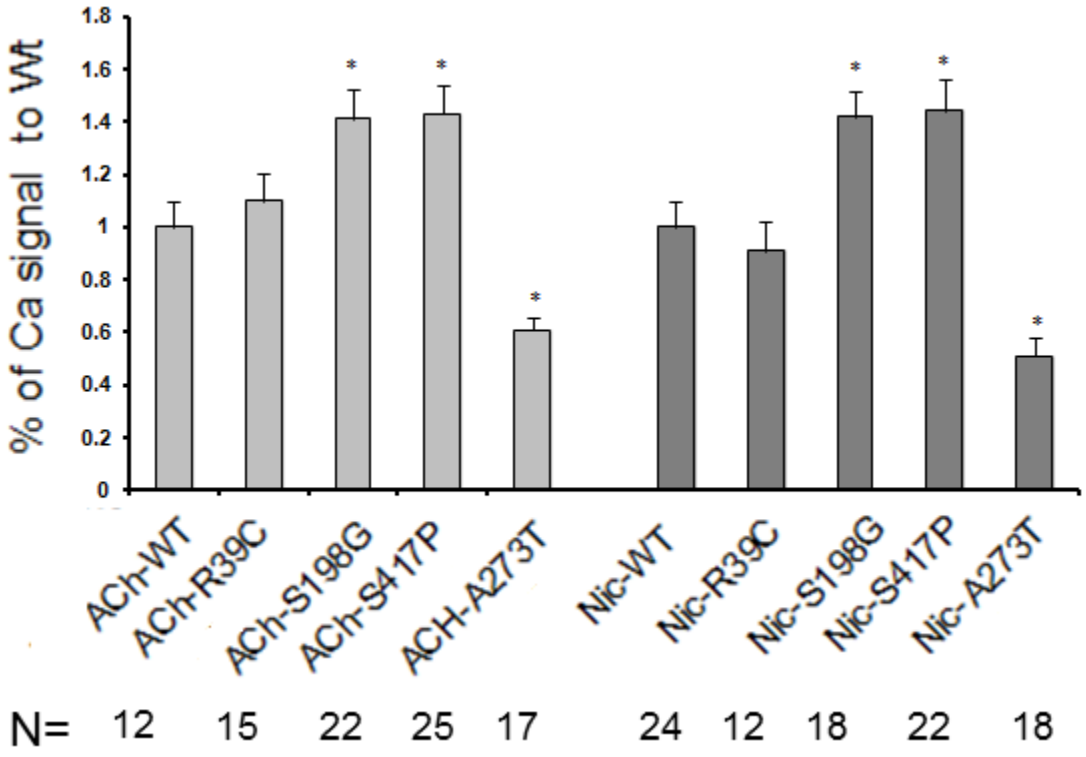

Figure 21: Effect of β4 subunit variants on tsa-201 Cells transfected with 1µg of WT α3 and 1µg WT β4 or 1µg mutant β4 plasmid on Calcium fluorescence signal in responding to 20µM ACH or NIC. The photos were treated and measured using Axon Imaging Workbench program (AIW2.2) to convert the signals to numbers. The columns show the average of maximum response to 20µM ACH or NIC. Significant differences, determined by two-tailed student's t test, are indicated (*, $P< 0.05$)

3.2. Rare Mutations were detected in the *Ric-3* gene.

3.2.1. Genetic screening of the *Ric-3* gene:

The *Ric-3* gene was comprehensively screened in 315 AF cases and 600 healthy controls. We observed an excess of rare variants in cases vs controls (Table 4). Four rare variants (K25R, V196F, S294L, and P299A) were detected only in AF cases but not in controls as shown in figure 22 and showed a difference in functional properties on nAChRs compared with WT. Two of these variants V196F and S294L also segregated with affected AF patients in small kindreds, as shown in Figure (23 A &B). Interestingly, V196F variant was also detected in one of the control cases. This control individual was contacted and conveyed that within the last year she had developed AF, which was not present at the time of her enrollment as a control patients years before.

Table 4: list of Ric-3 variants that detected by comprehensive screening of *Ric-3* gene in 300 AF patients and 615 controls.

Variants	Exon	Patients (320) Number	%	Control Subjects (N=615) Number	%	Functional study
K25R	1	3	0.95	0	0	Gain of function
g-a promoter SNP	1	11	3.50	0	0	nt
Pro101Ser	2	2	0.62	2	0.36	nt
Ile102Leu	2	0	0	1	0.18	nt
Gly104Ser	2	0	0	1	0.18	nt
Ile99Ile snp	2	2	0.62	0	0	nt
Cys130Tyr	3	40	12.4	64	10.39	nt
P135S	3	22	6.81	47	7.91	nt
Ala121Gly	3	8	2.48	9	1.52	nt
val168val	4	1	0.31	0	0	nt
Val196Phe *	5	1	0.31	1**	0.17	Gain of function
Glu-Glu + intronic frameshift	5	3	0.94	0	0	nt
D351N	6	39	12.2	68	11.07	nt
D311N	6	4	1.25	0	0	No difference
Pro299Arg	6	1	0.31	0	0	Gain of function
Ser294Leu *	6	1	0.31	0	0	Gain of function

** This control has AF; * family segregation; nt= not tested; gain of function= increase the surface and functional expression compared to Wt.

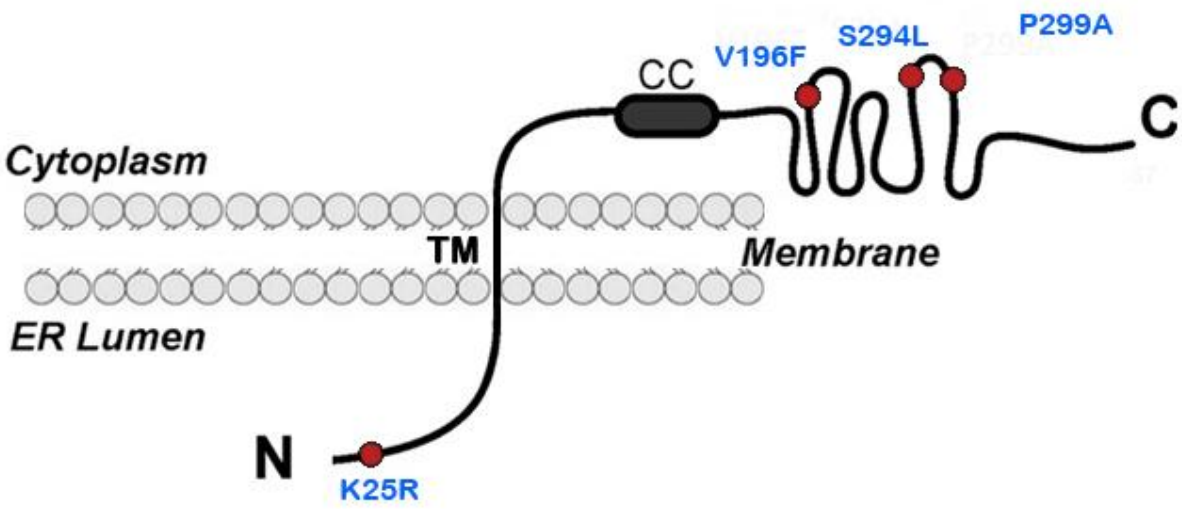

Figure 22: A schematic diagram of Ric-3 protein comprises an N-terminal domain exposed to the ER compartment, a membrane-spanning domain, coiled-coil domain (CC), and a C-terminal domain exposed to the cytoplasmic compartment.K25R mutation located on the N-terminal domain, V196F, S294L, and P299A mutations located on the C-terminal domain.

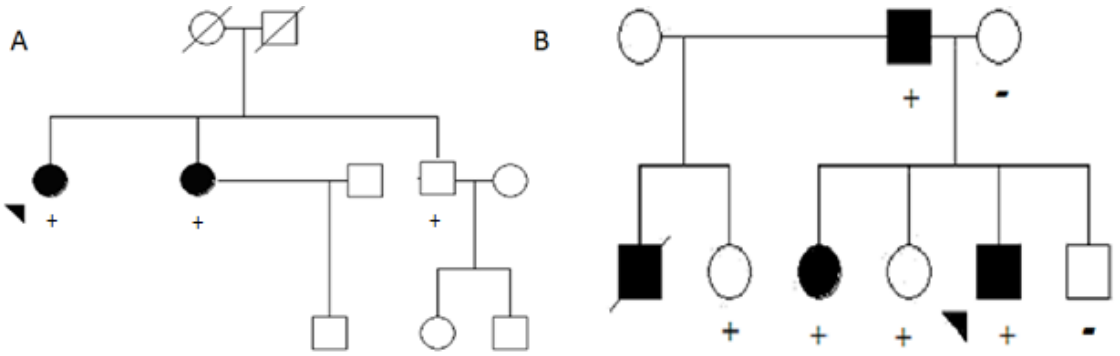

Figure 23: **Pedigree structures of a family with atrial fibrillation and segregate V196F (A) & S294L (B)**. Squares indicate male family members; circles, female members; symbols with a slash, the deceased members; closed symbols, affected members; open symbols, unaffected members; arrow, proband; ; '+', has the variant; -, has not the variant.

3.2.2. Ric-3 effects on the functional expression of nAChRs in HEK 293 α3β4α5 stably transfected cells.

3.2.2.1. Mutated Ric-3 enhances the cell's current density compared to Wt.

The effect of Ric-3 variants on the functional expression of nAChRs in HEK 293 α3β4α5 stably transfected cells was studied by the whole cell patch clamp technique. Application of 10μM ACH to cells transiently transfected with rare Ric-3 mutants (K25R, V196F, S294L, or P299A) evoked significantly enhanced currents, as compared to WT transfected cells and untransfected cells, as shown in Figure 24 A. Normalized currents density for cells elicited upon application of 10μM ACH for cells transfected with CMV plasmid without Ric-3, Ric-3 WT, K25R, V196F, S294L, or P299A are summarized in Figure 24 B.

The same experiments were performed to determine the evoked currents by application of 1mM NIC to patch clamped HEK 293 stably transfected cell with α3, β4, and α5 and transient transfected with Ric-3 WT or variants, and similarly significantly increased currents, as shown in Figure 24 C. Normalized currents density for cells elicited upon application of 1mM NIC for cells transfected with CMV plasmid without Ric-3, Ric-3 WT, K25R, V196F, S294L, or P299A are summarized in Figure 24 D. These results indicate that the observed rare Ric-3 variants significantly enhance the functional expression of α3β4α5-nAChRs. This may be secondary to either an increase the number of nAChRs expressed at the cell surface or by direct biophysical effects on channel kinetics. To answer this question we first tested the sensitivity of the nAChRs in cells transfected with variants or WT Ric-3.

EC50 Dose-Response

To determine the receptor sensitivity and the effect of Ric-3 variants on EC50 we studied the ACH and Nic dose- response relationship, the results shown in figure (25 A &B). There were no significant differences in sensitivity of the nAChRs in cells transfected with any of mutated Ric-3 clones as compared to cells transfected with WT Ric-3. Thus, enhanced α3β4α5-nAChRs was not due to increased sensitivity to ligand in the presence of mutant Ric-3 clones. We next assessed whether or not mutant Ric-3 enhances the surface expression of nAChRs. This was tested 2 ways, by radioligand assay and immunoblotting techniques (results in section **3.2.3)**.

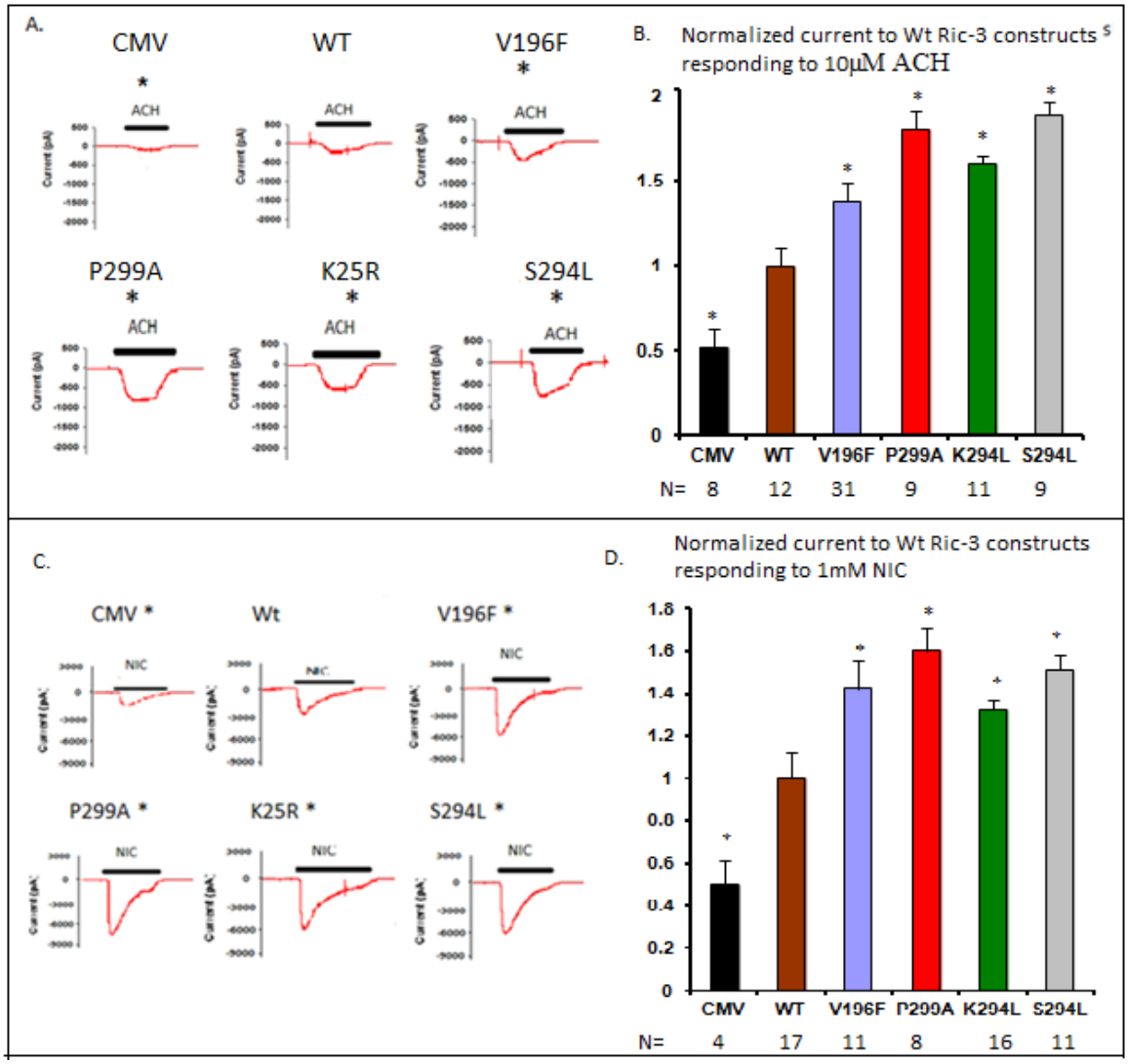

Figure 24: Four variants significantly enhance the functional expression of α3α5β4 nAChR detected by whole cell current in Response to 10µM ACH.(A) Representative traces of currents elicited upon application of 10µM ACH from HEK 293 α3β4α5 stably transfected cell and co transfected with 100ng Ric-3 WT, Ric-3 Variants, and CMV plasmid. (B)Normalized currents density for cells elicited upon application of 10µM ACH. Bars indicate time of ACH application. Numbers of N in figure A are respectively, Empty CMV (n= 8), WT (n=38), V196F (n=31), P299A (n=9), K25R (n=11), and S294L (n=9). (C) Representative traces of currents elicited upon application of 1µM NIC from HEK 293 α3β4α5 stably transfected cell and co transfected with 100ng Ric-3 WT, Ric-3 Variants, and CMV plasmid (D) Normalized currents density for cells elicited upon application of 1mM NIC, Numbers of N in figure C are respectively, Empty CMV (n= 4), WT (n=17), V196F (n=11), P299A (n=8), K25R (n=16), and S294L (n=11). Significant differences, determined by two-tailed student's t test, are indicated (*, P< 0.05)

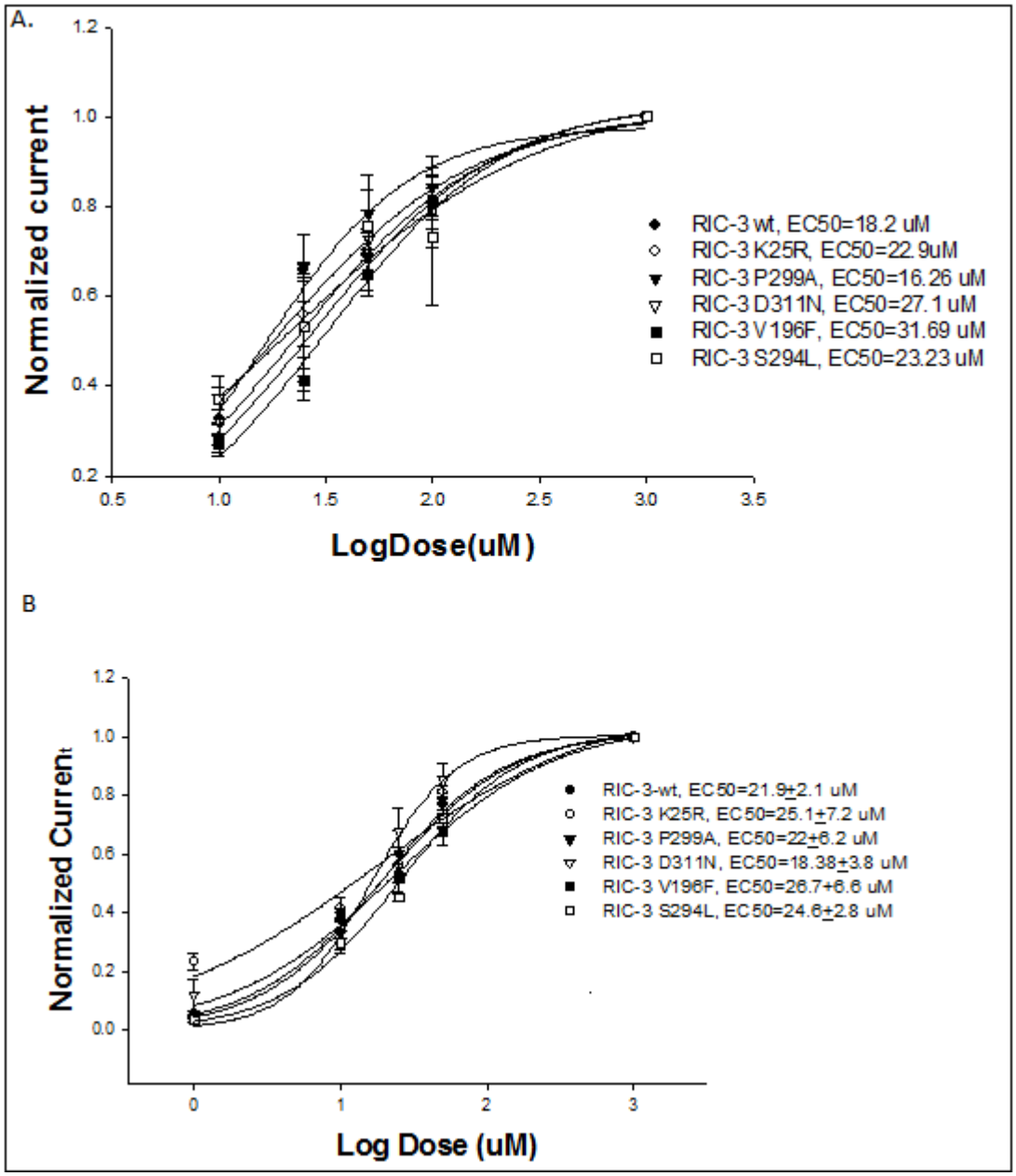

Figure 25: The dose-response relationships for HEK 293 α3β4α5 stably transfected cell and co transfected with 100ng Ric-3 WT and Variants in response to ACH (A) and NIC (B). The currents are plotted as a function of the logarithmic scale of the ACH concentration (A) and NIC concentration (B). Values are normalized to the maximal current evoked by the highest ACH or NIC concentration. Curves through the data were created as the best fit to the Hill equation. Error bars indicate the standard error of the mean.

3.2.2.2. Mutated Ric-3 enhances the Calcium fluorescence signal response to ACH and NIC compared to WT.

Calcium intracellular signal responses to ACH and NIC were measured from HEK 293 stably expressed cells with α3, β4, and α5 and transiently transfected with Ric-3 WT or variants. These signals were detected by taking photos every 2 seconds before, during, and after applying 20 µM ACH or 5 µM NIC. Figure 26 shows photos taken for the signal during the cell response 20 µM ACH Figure 26 A and to 5 µM NIC Figure 26 B.

The results showed a significant increase in the intracellular calcium signal responding to ACH and NIC respectively in cells transfected with WT Ric-3 compared to the cells without Ric-3 as shown in Figure 27 A. These results are consistent with previously reported data in heteromeric nAChRs as reported by Lansdell, S. J., et al. 2005. For variant Ric-3 clones, Ric-3 variants K25R, V196F, S294L, and P299A significantly enhanced the intracellular Ca signals compared to WT, indicating that these variants enhance the functional expression of nAChRs compared to Wt. Figure 27 B&C summarizes the results of response to ACH and NIC respectively as the fluorescence were analyzed and measured using Axon Imaging Workbench program (AIW2.2).

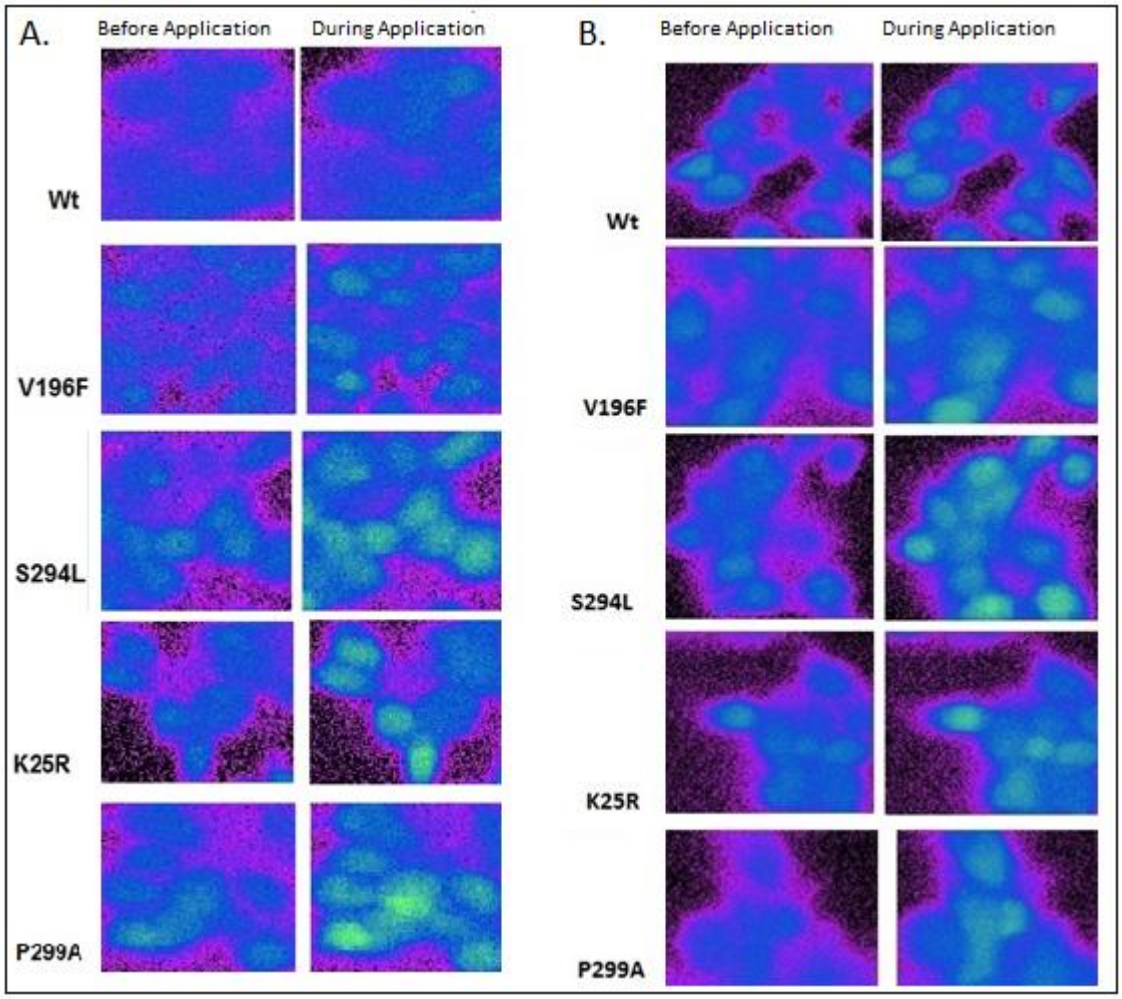

Figure 26: **Mutant Ric-3 Enhance the Calcium fluorescence signal in responding to 20ηM ACH or 5μM NIC**. HEK 293 α3β4α5 stably transfected cell and co transfected with 100ng Ric-3 plasmid, loaded with 5μM Ca green1/am dye for 70 min. the calcium signal was recorded by Monochrome CCD Camera (Cohu Inc, Poway CA). the recording performed before, during, and after add 20ηM ACH (A) and 5μM NIC (B). Left Photos represent the base line response of cell before ACH or NIC added, Right Photos represent the cell responding to 20ηM ACH (A) or 5μM NIC (B).

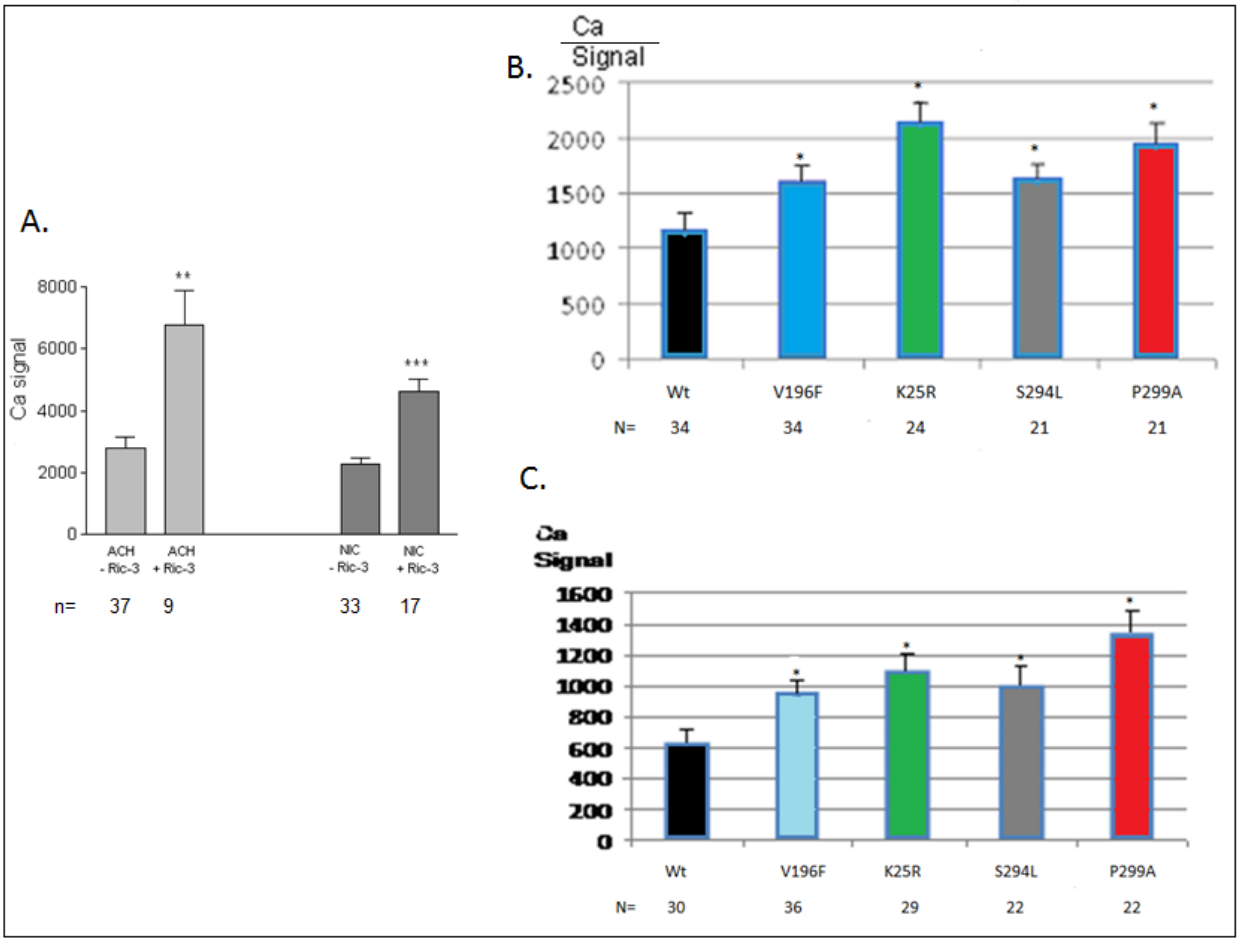

Figure 27: **Mutant Ric-3 Enhance the Calcium fluorescence signal in responding to 20µM ACH and 5µM NIC**. The photos were treated and the fluorescence was measured using Axon Imaging Workbench program (AIW2.2) to convert the signals to numbers. (A) The columns show the average of maximum response to 20µM ACH and 5µM NIC respectively to cells transfected with (+Ric-3) or without (-Ric-3). (B) The columns show the average of maximum response to 20µM ACH as following, black (WT), blue (V196F), green (K25R), gray (S294L), and red (P299A). (C) The columns show the average of maximum response to 5µM NIC as following, black (WT), blue (V196F), green (K25R), gray (S294L), and red (P299A). Significant differences, determined by two-tailed student's t test, are indicated (*, $P < 0.05$)

3.2.3. Ric-3 effects on the surface expression of nAChRs in HEK 293 α3β4α5 stably transfected cells.

3.2.3.1. Mutated Ric-3 enhances the surface expression of nAChRs in HEK 293 α3β4α5 stably transfected cell as indicated by [3H]-Epibatidine specific binding assay:

The surface expression of nAChRs in cells transfected with one of the three Ric-3 variants (S294L, K25R, and P299A) significantly enhanced the specific [^{3}H]-Epibatidine binding using 35ηM of [^{3}H]-Epibatidine compared to cells transfected with WT Ric-3, as shown in Figure 28. The results indicate that the number of functional receptors on the cell surface increased significantly in cells transfected with mutant Ric-3 as compared to those transfected with WT Ric-3, indicating that mutant Ric-3 resulted in increased trafficking of the nAChRs subunits from the ER to the cell surface.

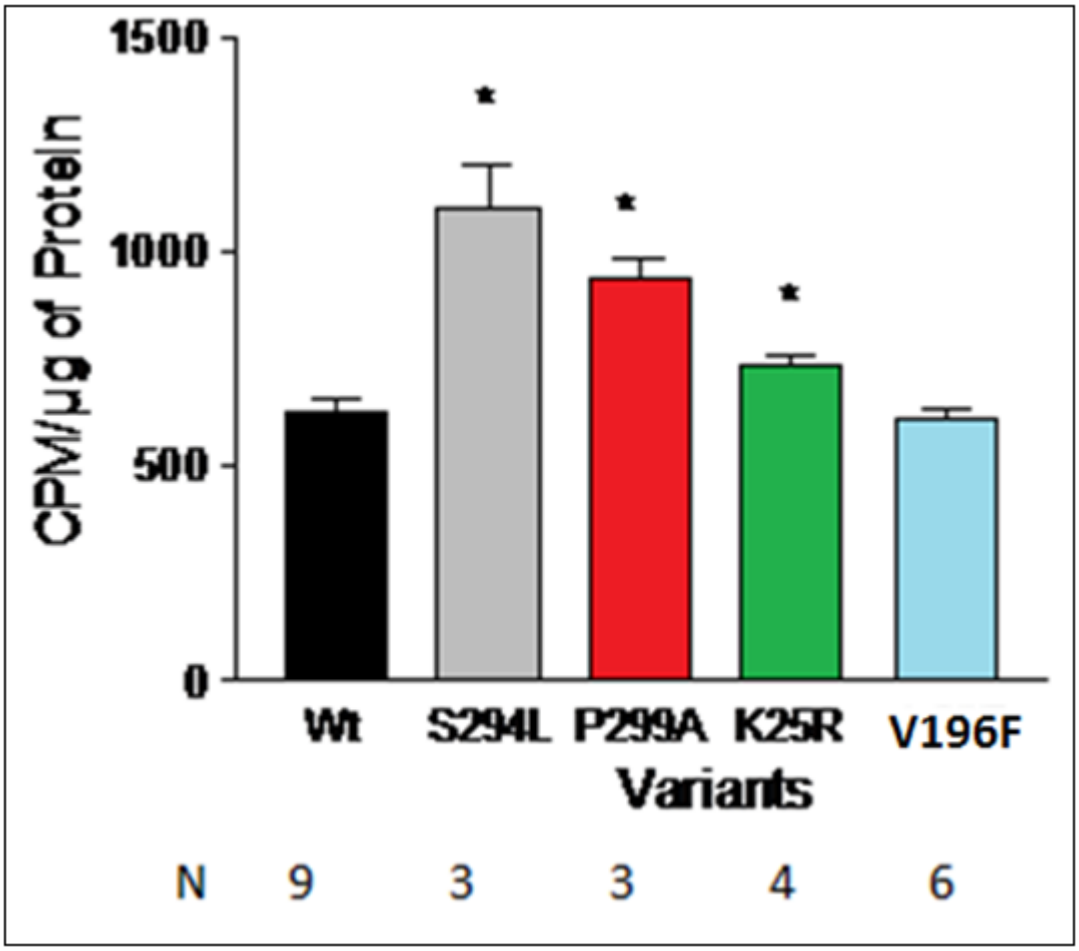

Figure 28: Influence of Ric-3 WT and variants on Specific [^{3}H]-Epibatidine binding using 35ηM of [^{3}H]-Epibatidine. Specific binding was determined with HEK 293 α3β4α5 stably transfected cell and co transfected with Ric-3 constructs. Data are means of three to nine independent experiments. Significant differences, determined by two-tailed student's t test, are indicated (*, P< 0.05)

3.2.3.2. Mutated Ric-3 enhances the surface expression of nAChRs in HEK 293 α3β4α5 stably transfected cell as indicated by Western blot technique:

The surface expression of nAChRs in HEK 293 stably transfected cells containing α3, β4, and α5 subunits, and transiently transfected with Ric-3 WT or variants was tested by subjecting extracted cell membrane preps to Western blotting to measure the level of α3 subunits. Membrane extracts were bound with specific anti-rabbit anti-α3 subunits or anti-mouse anti-CFP antibody to measure Ric-3-CFP fused protein. For the loading control we bound the membranes with anti-mouse anti-TFR antibody (transferrin receptor).

The results showed a significant increase in the level α3 subunits protein on the surface of cells transfected with mutated Ric-3; K25R, V196F, S294L, and P299A as compared to levels in cells transfected with WT Ric-3, as shown in Figure 29 A. Immunoblots were quantified and normalized to TFR levels as shown in Figure 29 B. The relative α3 subunit protein levels normalized to TFR were significantly increased in cells transfected with K25R, V196F, S294L, and P299A as compared to the cells with Ric-3 WT. This data further supports that mutant Ric-3 increased the receptor number at the cell surface. No significant difference was observed for each experiment in the relative Ric-3 protein level normalized to TFR, as shown in Figure 29 C, indicating that total level of Ric-3 or protein loading differences did not affect the immunoblotting result.

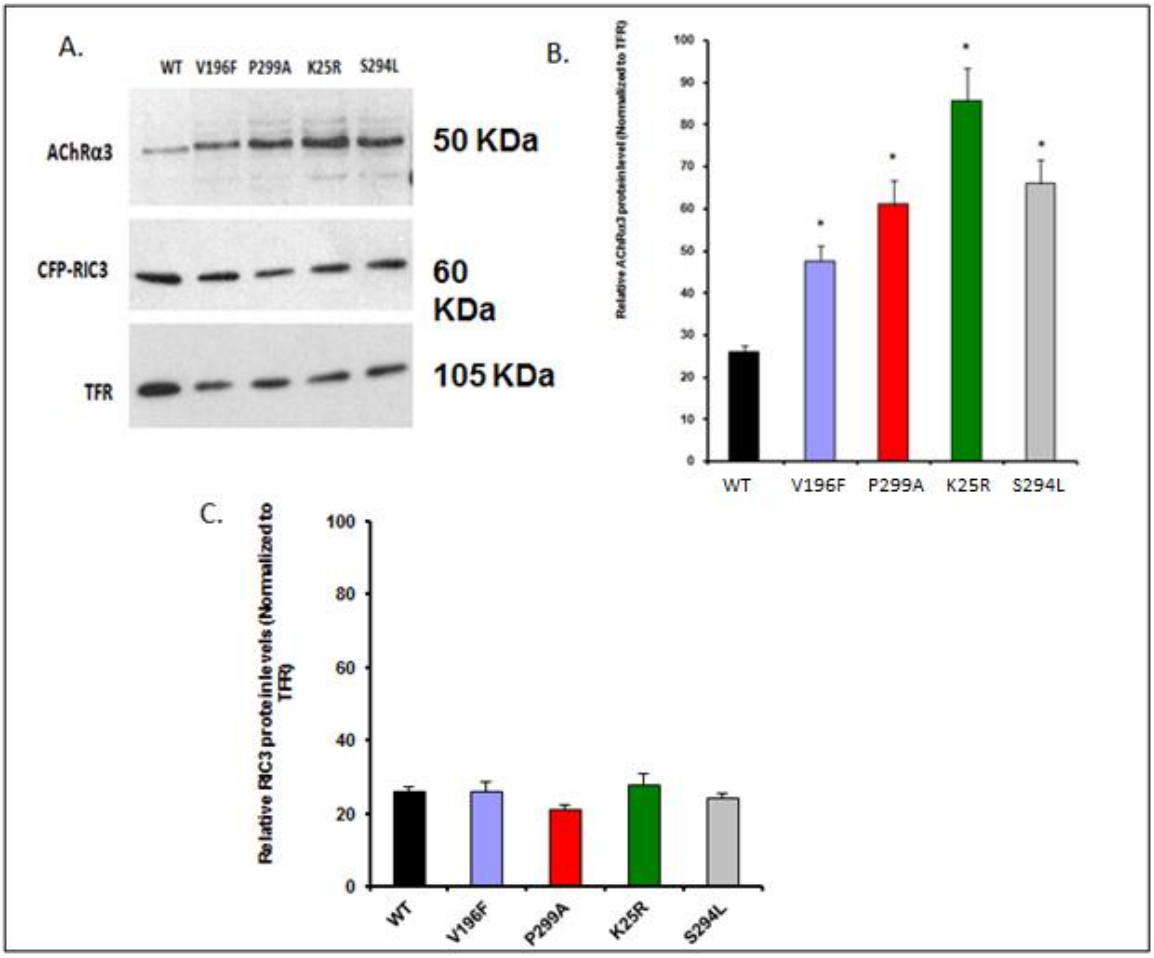

Figure 29: **Ric-3 Variants enhance the level of α3 subunits of nAChR protein compared to the Ric-3 Wt**. (A) Western blot analysis of α3 subunits of nAChR and Ric-3 WT and Variants of membranes collected from HEK 293 α3β4α5 stably transfected cell and co transfected with Ric-3 constructs. Cells were harvested 36-48 hours after transfection, the membranes were collected and separated by SDS-PAGE following by blotting with anti α3 subunits of nAChR anti body, anti CFP antibody for detection of Ric-3 fused with cfp fluorescence protein, and anti Transferrin receptor (TFR) antibody for loading control. (B) Represent Relative AChRα3 protein level normalized to TFR. (C) Relative Ric-3 protein levels normalized to TFR.

4. Discussion:

4.1. Rare Mutations in the *CHRNB4* gene cause significant differences in the biophysical function in alpha3-B4-nAChRs.

In only the last decade has knowledge been gained on the specific genetic factors that may predispose to AF. This deeper understanding explains the etiology in many previously believed 'idiopathic' cases, and brings forth the opportunity to design more specific anti-arrhythmic therapies based on the elucidated mechanisms. In this research, we explored a novel pathway that may predispose individuals to AF, specifically the molecular mediators of the parasympathetic or cholinergic signalling on the heart.

The autonomic nervous system is well-accepted to play a very important role in the occurrence of AF (Zimmermann, M. 2003). Since the first description of vagal AF by Phillipe Coumel in 1978, modern day electrophysiologists continue to focus on the role of the autonomics in arrhythmogenesis. Current therapeutic procedures often target regions of the heart where peripheral ganglia are believed to reside, in the hope of modifying parasympathetic inputs to the heart and to diminish AF recurrence.

The molecular mediators of autonomic input to the heart and other organs are nAChRs, which reside on post-ganglionic nerve fibres, bind ACH and then rapidly transmit cholinergic signalling to the myocardium (Devay, P., et al. 1999). The distribution of the subunits that comprise functional, pentameric nAChRs in different tissues depends on the diversity of nAChRs gene expression (Skok, V. I. 2002). The main mediators of fast synaptic transmission in cardiac ganglia are nAChR comprised of the α3β4 subtype, which are known to be highly expressed in the autonomic ganglia of the

peripheral nervous system where they transduce cholinergic transmission at the synapses in the peripheral ganglia (Bibevski, S., et al. 2000; De Biasi, M. et al., 2002). In a prior approach, our lab comprehensively screened the *CHRNA3* gene which encodes for α3 subunit of nAChR in 300 AF patients, and did not find any significant number of rare genetic variants in this gene (data not shown). Therefore, in this current research project, genetic screening of the *CHRNB4* gene that encodes for β4 subunits of nAChR was performed. We hypothesized that genetic defects in *CHRNB4* may create a vulnerability to AF by enhancing 'vagal' sensitivity, making some patients hypersensitive to vagal scenarios leading to exaggerated electrophysiological changes. As noted in the introduction of this thesis, CHRNB4 is a particularly attractive candidate to consider as a gene that may modify vagal response on the heart, as knock out mice of this gene demonstrate attenuated vagal response (Wang, N., et al. 2002).

For functionally characterizing the behaviour of rare variants identified in patients, we used HEK tsa-201 cells, a naive cell line that does not express nAChR subunits, and is a cell line proven to be a robust and reliable platform for expressing receptor proteins and ion channels with high fidelity (Thomas, P., et al. 2005).

In our study, four of five mutations detected in AF patients but not in the controls cases showed significant differences in biophysical function, including alterations in receptor current density and sensitivity in response to neuroligand. Both mutations S417P and S198G in nAChRs caused an increase in maximum current evoked by Ach compared to WT, in addition to loss of receptor desensitization. T273A mutation caused a decrease in maximum current evoked by Ach, but showed findings consistent with S417P and S198G in demonstrating a decreased rate of desensitization. Although the R39C mutation showed

no difference in maximum current compared to WT, this mutant also showed a decrease of receptor desensitization. Although variations of altered function was observed in these 4 variants, they all shared the common observation of decreased or loss of receptor desensitization.

Desensitization of a channel or receptor refers to the waning responsiveness to agonist with time, and is believed to represent an important physiological feedback mechanism that protects against both acute and chronic receptor overstimulation (Gainetdinov, R. R., et al. 2004; Hausdorff, W. P., et al. 1990). This phenomenon has traditionally been viewed in the context of adaptation, wherein the receptor system enters a refractory state in the presence of sustained ligand stimuli and thereby prevents the cell or target organ from over-responding to the ligand. Our data indicating a loss of alpha3-beta4-nAChR desensitization implies that the observed genetic variants may impart a 'hypersensitive' cholinergic signalling state, making some patients prone to an exaggerated cardiac vagal response under routine stimuli or in the resting state. During sleep for example, a common scenario for AF onset in healthy individuals, a 'hypersensitive' vagal signalling system may lower the threshold for AF vulnerability due to exaggerated electrophysiological substrate changes. It would be reasonable to expect that loss of nAChR desensitization may have an effect on the magnitude of the response to repetitive ligand inputs or during natural shifts in the balance between sympathetic-parasympathetic influences.

Electron microscopy studies of nAChR suggest three distinct domains of nAChRs; the extracellular domain (ECD), the transmembrane domain (TMD) and a cytoplasmic, intracellular domain. (Taly, A., et al. 2009; Parker, M. J., et al. 2001). The binding site for ACH lies within the ECD and contains several amino acids residues (Asn55, Val56,

E63T) that contribute to ligand binding (Parker, M. J., et al. 2001; Taly, A., et al. 2009). In addition, Lindovsky and colleagues have provided data indicating that the ECD also contains residues that may affect the kinetics of desensitization (Lindovsky, J., et al. 2008). These investigators, using a structure-function approach, identified that altering residues Asp191 (to Asn) and Asp192 (to Asn) in CHRNB4 resulted in slower desensitization of the receptor. Our Ser198Gly mutation, which demonstrated significantly delayed desensitization is in close vicinity, further implicating this region of the ECD in regulating channel kinetics. The role of more N-terminal amino acid residues in the region of our detected R39C mutation is less clear. Although structure-function studies of the beta4 subunit of nAChRs are scarce, studies in this family of receptors also suggest an important role of the large cytosolic, intracellular domain in regulating receptor desensitization (Zhang, J., et al. 2013). Our data on the observed rare Ser417Pro mutation would support a role of this domain in regulating desensitization.

In conclusion, we demonstrate that rare mutations in the CHRNB4 gene may be identified in a proportion of AF patients, and that these variants impart a loss of receptor desensitization, potentially setting the stage for a 'hypersensitive' cholinergic signalling system.

4.2. Ric-3 enhances the functional expression of nAChRs.

The Ric-3 protein was first recognized as protein that facilitates functional expression of nAChRs. Studies in xenopus and mammalian cells have confirmed that co-expression of Ric-3 with nAChR subunits regulates nAChR function, as measured by current density and cell surface expression studies (Williams, M. E., et al. 2005; Lansdell, S. J., et al.

2005). Interestingly, there appears to be a fine balance to Ric-3 expression levels in the regulation of functional nAChRs (Alexander, J. K., et al. 2010). Alexander and colleagues demonstrated that in mammalian cells, Ric-3 levels increased nAChR function and cell surface expression to a limit (Alexander, J. K., et al. 2010). Increasing Ric-3 levels beyond a certain threshold then negates this effect and results in a decrease nAChR cell surface expression (Alexander, J. K., et al. 2010). Accordingly, in light of Ric-3's role in regulating nAChR function and thereby presumably autonomic tone and physiology, we genetically screened the human Ric-3 gene in our 315 AF and 600 control cohorts. The results were intriguing and revealed an abundance of rare Ric-3 variants in our AF patients, $p<0.02$ for comparison of rare variant frequency.

Among the detected variants, four rare variants were detected in AF patients but not in controls subject. Those variants were K25R, V196F, S294L, and P299A. Two of these variants, V196F and S294L, segregated with affected status in 2 small kindreds. The V196F variant was also detected in one of the control cases. When this patient was contacted she acknowledged a recently documented history of AF, which was confirmed on retrieval of her 12-lead ECGs.

In our Ric-3 study, we used HEK293 cells that are stably expressing α3β4α5 nAChRs. This composition of subunits are the most abundant in peripheral autonomic ganglia (Wang, N., et al. 2002; Nelson, M. E., et al. 2001; Chavez-Noriega, L. E., et al. 1997). These cells prevented the need to perform transfections of multiple cDNA clones simultaneously. We confirmed that expression of WT Ric-3 into these cells promotes increased functional expression of α3β4α5 nAChRs. Similarly, intracellular calcium response to both NIC and ACH also showed a significant increase in cells transfected

with WT Ric-3 plasmid compared to untransfected cells. Our results were consistent with previously reported data that Ric-3 enhances the functional expression of nAChRs (Millar, N. S. 2008; Lansdell, S. J., et al. 2005). We next assessed the effect of rare variants in Ric-3 on these experimental assays.

We have demonstrated that four of five rare variants (K25R, V196F, S294L, and P299A) caused a gain-of-function in α3β4α5 nAChR, as compared to WT Ric-3. Both current density and intracellular calcium response to ligand was significantly increased for mutant Ric-3. We then demonstrated, using 2 independent approaches of radioligand binding and cell membrane immunoblotting, that this was due to increased surface expression of α3β4α5 nAChR's.

It remains unclear how mutant Ric-3 facilitated functional surface expression of α3β4α5 nAChR's, and what the specific effects of observed mutations in Ric-3 are on Ric-3 function. As noted above, previous data suggests that Ric-3 levels may be relevant in regulating assembly and trafficking of nAChR subunits, and that above a certain level of Ric-3 expression in the cell the ability of Ric-3 to enhance nAChR functional expression is reversed. Using the nAChR analogue, the bungarotoxin receptor (BgtR), Alexander and colleagues showed that at relatively higher levels of Ric-3, the surface delivery of nAChRs was suppressed, but not its assembly and the BgtR was retained in the ER by Ric-3- containing aggregation (Alexander, J. K., et al. 2010). Thus, it is possible that the observed Ric-3 mutants led to a loss of function (eg. self-aggregation or degradation) in Ric-3, effectively reducing the steady-state level of this active nAChR chaperone and adjusting Ric-3 levels to a more optimal concentration for nAChR interactions leading to enhanced assembly and trafficking. Alternatively, these mutations

themselves may enhance interactions with nAChR subumits facilitating their chaperoning capacity. Further experiments using electron microscopy for assessment of Ric-3 localization or aggregation, or tracer studies to follow the assembly and trafficking pathway of nAChR subunits may provide insight into these possibilities.

It is important to recognize the limitations of our study. First and foremost, the genetic observations in no way provide evidence of absolute causality of AF in affected patients. Causality is best established through segregation of rare variants with multiple affected individuals in a large family. At most, our observations may suggest that these rare variants are contributory to AF development in these patients, assuming multifactorial or polygenic influences. These results are exploratory and represent a proof-of-concept that genetic variants in nAChRs or their chaperone Ric-3 may alter physiology in a way consistent with enhanced cholinergic signalling. Importantly, our studies were performed in vitro, outside of the influences of an intact and integrated neuro-hormonal axis as would be relevant in human subjects. Future studies may be aimed at creating knock-in mice models of the specific mutations and assessing the effect on cholinergic signalling to the heart. However, such studies may be challenging in rodent models due to their naturally high sympathetic tone. Lastly, numerous other molecular mediators (enzymes, co-factors, etc) exist that modulate autonomic function and genetic evaluation of these other factors may shed further insight.

4.3. Summary and Conclusion:

In this thesis we investigated the novel question of the potential role of nicotinic acetylcholine receptors (nAChRs), molecular mediators of autonomic tone of the heart, in human AF. We used a combined approach of genetic, biophysical, calcium imaging, radioligand and immunoblotting studies to characterize the physiological effects of rare mutations in genes involved in cholinergic signalling. We provide data for the first time on the functional effect of rare mutations of the *CHRNB4* and *Ric-3* genes identified in patients with AF. Our data indicates that rare variants in these genes lead to enhanced nAChR function, and raises the possibility that genetic defects in genes encoding the molecular mediators of parasympathetic tone in the heart may contribute to the well-known subtype of AF known as 'vagal AF'. Although this data should be considered as preliminary and hopefully provoke further studies in this area, the data has potential far reaching implications for novel approaches to pharmacologic modulation in AF patients. It is conceivable that anti-arrhythmic therapy targeting specific subtypes of nAChRs may succeed in modulating autonomic tone in those patients experiencing clear vagal-related AF events.

5. References:

Albuquerque, E. X., et al. (2009). "Mammalian nicotinic acetylcholine receptors: from structure to function." Physiol Rev **89**(1): 73-120.

Alexander, J. K., et al. (2010). "Ric-3 Promotes α7 Nicotinic Receptor assembly and trafficking through the ER sub compartment of dendrites." J Neurosci **30**(30):10112-10126.

Almontashiri, N. A., et al. (2013). "Interferon-gamma activates expression of p15 and p16 regardless of 9p21.3 coronary artery disease risk genotype." J Am Coll Cardiol **61**(2): 143-147.

Ben-Ami, H. C., et al. (2005). "RIC-3 affects properties and quantity of nicotinic acetylcholine receptors via a mechanism that does not require the coiled-coil domains." J Biol Chem **280**(30): 28053-28060.

Benjamin, E. J., et al. (1998). "Impact of atrial fibrillation on the risk of death: the Framingham Heart Study." Circulation **98**(10): 946-952.

Bertrand, D., et al. (2002). "How mutations in the nAChRs can cause ADNFLE epilepsy." Epilepsia **43** Suppl 5: 112-122.

Bibevski, S., et al. (2000). "Functional nicotinic acetylcholine receptors that mediate ganglionic transmission in cardiac parasympathetic neurons." J Neurosci **20**(13): 5076-5082.

Borghese, C. M., et al. (2002). "Acetylcholine and alcohol sensitivity of neuronal nicotinic acetylcholine receptors: mutations in transmembrane domains." Alcohol Clin Exp Res **26**(12): 1764-1772.

Braunwald, E. (1997). "Shattuck lecture--cardiovascular medicine at the turn of the millennium: triumphs, concerns, and opportunities." N Engl J Med **337**(19): 1360-1369.

Brugada, R., et al. (1997). "Identification of a genetic locus for familial atrial fibrillation." N Engl J Med **336**(13): 905-911.

Burn, J. H. (1979). "Excitatory actions of acetylcholine in the heart." Br J Pharmacol **67**(1): 3-12.

Carlsson, L., et al. (2010). "New pharmacological targets and treatments for atrial fibrillation." Trends Pharmacol Sci **31**(8): 364-371.

Castelan, F., et al. (2008). "Molecular characterization and localization of the RIC-3 protein, an effector of nicotinic acetylcholine receptor expression." J Neurochem **105**(3): 617-627.

Castillo, M., et al. (2005). "Dual role of the RIC-3 protein in trafficking of serotonin and nicotinic acetylcholine receptors." J Biol Chem **280**(29): 27062-27068.

Champtiaux, N. and J. P. Changeux (2002). "Knock-out and knock-in mice to investigate the role of nicotinic receptors in the central nervous system." Curr Drug Targets CNS Neurol Disord **1**(4): 319-330.

Champtiaux, N., et al. (2003). "Subunit composition of functional nicotinic receptors in dopaminergic neurons investigated with knock-out mice." J Neurosci **23**(21): 7820-7829.

Changeux, J. P. (2012). "The nicotinic acetylcholine receptor: the founding father of the pentameric ligand-gated ion channel superfamily." J Biol Chem **287**(48): 40207-40215.

Changeux, J. and S. J. Edelstein (2001). "Allosteric mechanisms in normal and pathological nicotinic acetylcholine receptors." Curr Opin Neurobiol **11**(3): 369-377.

Changeux, J. P. and S. J. Edelstein (1998). "Allosteric receptors after 30 years." Neuron **21**(5): 959-980.

Chavez-Noriega, L. E., et al. (1997). "Pharmacological characterization of recombinant human neuronal nicotinic acetylcholine receptors h alpha 2 beta 2, h alpha 2 beta 4, h alpha 3 beta 2, h alpha 3 beta 4, h alpha 4 beta 2, h alpha 4 beta 4 and h alpha 7 expressed in Xenopus oocytes." J Pharmacol Exp Ther **280**(1): 346-356.

Chen, Y. H., et al. (2003). "KCNQ1 gain-of-function mutation in familial atrial fibrillation." Science **299**(5604): 251-254.

Ben-Ami, H. C., et al. (2005). "RIC-3 affects properties and quantity of nicotinic acetylcholine receptors via a mechanism that does not require the coiled-coil domains." J Biol Chem **280**(30): 28053-28060.

Corringer, P. J., et al. (2012). "Structure and pharmacology of pentameric receptor channels: from bacteria to brain." Structure **20**(6): 941-956.
Costa, V., et al. (2003). "A structural model of agonist binding to the alpha3beta4 neuronal nicotinic receptor." Br J Pharmacol **140**(5): 921-931.

Coumel, P., et al. (1978). "[The atrial arrhythmia syndrome of vagal origin]." Arch Mal Coeur Vaiss **71**(6): 645-656.

Coumel, P. (1994). "Paroxysmal atrial fibrillation: a disorder of autonomic tone?" Eur Heart J **15** Suppl A: 9-16.

Coyne, K. S., et al. (2006). "Assessing the direct costs of treating nonvalvular atrial fibrillation in the United States." Value Health **9**(5): 348-356.

Darbar, D., et al. (2003). "Familial atrial fibrillation is a genetically heterogeneous disorder." J Am Coll Cardiol **41**(12): 2185-2192.

Darbar, D. (2008). "Genetics of atrial fibrillation: rare mutations, common polymorphisms, and clinical relevance." Heart Rhythm **5**(3): 483-486.

De Biasi, M. (2002). "Nicotinic mechanisms in the autonomic control of organ systems." J Neurobiol **53**(4): 568-579.

Devay, P., et al. (1999). "Target-specific control of nicotinic receptor expression at developing interneuronal synapses in chick." Nat Neurosci **2**(6): 528-534.

D'Hoedt, D. and D. Bertrand (2009). "Nicotinic acetylcholine receptors: an overview on drug discovery." Expert Opin Ther Targets **13**(4): 395-411.

Dobrev, D., et al. (2001). "Molecular basis of downregulation of G-protein-coupled inward rectifying K(+) current (I(K,ACh) in chronic human atrial fibrillation: decrease in GIRK4 mRNA correlates with reduced I(K,ACh) and muscarinic receptor-mediated shortening of action potentials." Circulation **104**(21): 2551-2557.

Elenes, S., et al. (2006). "Desensitization contributes to the synaptic response of gain-of-function mutants of the muscle nicotinic receptor." J Gen Physiol **128**(5): 615-627.

Ellinor, P. T., et al. (2003). "Locus for atrial fibrillation maps to chromosome 6q14-16." Circulation **107**(23): 2880-2883.

Ellinor, P. T., et al. (2005). "Familial aggregation in lone atrial fibrillation." Hum Genet **118**(2): 179-184.

Fenster, C. P., et al. (1997). "Influence of subunit composition on desensitization of neuronal acetylcholine receptors at low concentrations of nicotine." J Neurosci **17**(15): 5747-5759.

Fischmeister, R. and H. C. Hartzell (1986). "Mechanism of action of acetylcholine on calcium current in single cells from frog ventricle." J Physiol **376**: 183-202.

Flegel, K. M., et al. (1987). "Risk of stroke in non-rheumatic atrial fibrillation." Lancet **1**(8532): 526-529.

Fox, C. S., et al. (2004). "Parental atrial fibrillation as a risk factor for atrial fibrillation in offspring." JAMA **291**(23): 2851-2855.

Gainetdinov, R. R., et al. (2004). "Desensitization of G protein-coupled receptors and neuronal functions." Annu Rev Neurosci **27**: 107-144.

Gallego, X., et al. (2012). "Overexpression of the CHRNA5/A3/B4 genomic cluster in mice increases the sensitivity to nicotine and modifies its reinforcing effects." Amino Acids **43**(2): 897-909.

Gavrilescu, S. and C. Luca (1975). "Right atrium monophasic action potentials during atrial flutter and fibrillation in man." Am Heart J **90**(2): 199-205.

Gee, V. J., et al. (2007). "Identification of domains influencing assembly and ion channel properties in alpha 7 nicotinic receptor and 5-HT3 receptor subunit chimaeras." Br J Pharmacol **152**(4): 501-512.

Gersh, B. J. and A. Solomon (1999). "Lone atrial fibrillation: epidemiology and natural history." Am Heart J **137**(4 Pt 1): 592-595.

Gollob, M. H., et al. (2006). "Somatic mutations in the connexin 40 gene (GJA5) in atrial fibrillation." N Engl J Med 354(25): 2677-2688.

Gotti, C. and F. Clementi (2004). "Neuronal nicotinic receptors: from structure to pathology." Prog Neurobiol 74(6): 363-396.

Gudbjartsson, D. F., et al. (2007). "Variants conferring risk of atrial fibrillation on chromosome 4q25." Nature 448(7151): 353-357.

Halevi, S., et al. (2002). "The C. elegans ric-3 gene is required for maturation of nicotinic acetylcholine receptors." EMBO J 21(5): 1012-1020.
Halevi, S., et al. (2003). "Conservation within the RIC-3 gene family. Effectors of mammalian nicotinic acetylcholine receptor expression." J Biol Chem **278**(36): 34411-34417.

Hart, R. G. and J. L. Halperin (2001). "Atrial fibrillation and stroke : concepts and controversies." Stroke **32**(3): 803-808.

Harvey, S. C. and C. W. Luetje (1996). "Determinants of competitive antagonist sensitivity on neuronal nicotinic receptor beta subunits." J Neurosci **16**(12): 3798-3806.

Hausdorff, W. P., et al. (1990). "Turning off the signal: desensitization of beta-adrenergic receptor function." FASEB J **4**(11): 2881-2889.

Heist, E. K. and J. N. Ruskin (2006). "Atrial fibrillation and congestive heart failure: risk factors, mechanisms, and treatment." Prog Cardiovasc Dis **48**(4): 256-269.

Hodgson-Zingman, D. M., et al. (2008). "Atrial natriuretic peptide frameshift mutation in familial atrial fibrillation." N Engl J Med **359**(2): 158-165.

Kannel, W. B., et al. (1991). "Belanger AJ. Epidemiology of heart failure." Am Heart J **121**:951–957.

Kedmi, M., et al. (2004). "Mice lacking neuronal nicotinic acetylcholine receptor beta4-subunit and mice lacking both alpha5- and beta4-subunits are highly resistant to nicotine-induced seizures." Physiol Genomics **17**(2): 221-229.

Kockskamper, J. and L. A. Blatter (2002). "Subcellular Ca2+ alternans represents a novel mechanism for the generation of arrhythmogenic Ca2+ waves in cat atrial myocytes." J Physiol **545**(Pt 1): 65-79.

Kovoor, P., et al. (2001). "Evaluation of the role of I(KACh) in atrial fibrillation using a mouse knockout model." J Am Coll Cardiol **37**(8): 2136-2143.

Krahn, A. D., et al. (1995). "The natural history of atrial fibrillation: incidence, risk factors, and prognosis in the Manitoba Follow-Up Study." Am J Med **98**(5): 476-484.

Kwak, B. R. and H. J. Jongsma (1996). "Regulation of cardiac gap junction channel permeability and conductance by several phosphorylating conditions." Mol Cell Biochem **157**(1-2): 93-99.

Lansdell, S. J., et al. (2005). "RIC-3 enhances functional expression of multiple nicotinic acetylcholine receptor subtypes in mammalian cells." Mol Pharmacol **68**(5): 1431-1438.

Lansdell, S. J., et al. (2008). "Host-cell specific effects of the nicotinic acetylcholine receptor chaperone RIC-3 revealed by a comparison of human and Drosophila RIC-3 homologues." J Neurochem **105**(5): 1573-1581.

Law, R. J., et al. (2005). "A gating mechanism proposed from a simulation of a human alpha7 nicotinic acetylcholine receptor." Proc Natl Acad Sci U S A **102**(19): 6813-6818.

Leier, C. V. and S. F. Schaal (1980). "Biatrial electrograms during coarse atrial fibrillation and flutter-fibrillation." Am Heart J **99**(3): 331-341.

Lemola, K., et al. (2008). "Pulmonary vein region ablation in experimental vagal atrial fibrillation: role of pulmonary veins versus autonomic ganglia." Circulation **117**(4): 470-477.

Le Novere, N. and J. P. Changeux (1995). "Molecular evolution of the nicotinic acetylcholine receptor: an example of multigene family in excitable cells." J Mol Evol **40**(2): 155-172.

Levy, S. (1998). "Epidemiology and classification of atrial fibrillation." J Cardiovasc Electrophysiol **9**(8 Suppl): S78-82.

Li, Y. F., et al. (2010). "Cytisine induces autonomic cardiovascular responses via activations of different nicotinic receptors." Auton Neurosci **154**(1-2): 14-19.

Liang, Y., et al. (2005). "Functional polymorphisms in the human beta4 subunit of nicotinic acetylcholine receptors." Neurogenetics **6**(1): 37-44.

Lim, P. B., et al. (2011). "Stimulation of the intrinsic cardiac autonomic nervous system results in a gradient of fibrillatory cycle length shortening across the atria during atrial fibrillation in humans." J Cardiovasc Electrophysiol **22**(11): 1224-1231.

Lindovsky, J., et al. (2008). "Role of negatively charged amino acids in beta 4 F-loop in activation and desensitization of alpha 3 beta 4 rat neuronal nicotinic receptors." Biochim Biophys Acta **1778**(4): 864-871.

Lindstrom, J. (2000). “The structures of neuronal nicotinic receptors”. In: Clementi F., Fornasari D., Gotti C. (Eds.), Handbook of Experimental Pharmacology Vol. Neuronal Nicotinic Receptors. Springer, Berlin, pp. 101–162.

Lloyd-Jones, D. M., et al. (2004). "Lifetime risk for development of atrial fibrillation: the Framingham Heart Study." Circulation **110**(9): 1042-1046.

Luetje, C. W. and J. Patrick (1991). "Both alpha- and beta-subunits contribute to the agonist sensitivity of neuronal nicotinic acetylcholine receptors." J Neurosci **11**(3): 837-845.

Lukas, R. J. and M. Bencherif (1992). "Heterogeneity and regulation of nicotinic acetylcholine receptors." Int Rev Neurobiol **34**: 25-131.

McNamara, R. L., et al. (2003). "Management of atrial fibrillation: review of the evidence for the role of pharmacologic therapy, electrical cardioversion, and echocardiography." Ann Intern Med **139**(12): 1018-1033.

Mahida, S., et al. (2011). "Monogenic atrial fibrillation as pathophysiological paradigms." Cardiovasc Res **89**(4): 692-700.

Mahida, S. and P. T. Ellinor (2012). "New advances in the genetic basis of atrial fibrillation." J Cardiovasc Electrophysiol **23**(12): 1400-1406.

Manyari, D. E., et al. (1990). "Atrial and ventricular arrhythmias in asymptomatic active elderly subjects: correlation with left atrial size and left ventricular mass." Am Heart J **119**(5): 1069-1076.

Markides, V. and R. J. Schilling (2003). "Atrial fibrillation: classification, pathophysiology, mechanisms and drug treatment." Heart **89**(8): 939-943.

Miyazawa, A., et al. (2003). "Structure and gating mechanism of the acetylcholine receptor pore." Nature **423**(6943): 949-955.

Millar, N. S. (2008). "RIC-3: a nicotinic acetylcholine receptor chaperone." Br J Pharmacol **153** Suppl 1: S177-183.

Nattel, S., et al. (2000). "Basic mechanisms of atrial fibrillation--very new insights into very old ideas." Annu Rev Physiol **62**: 51-77.

Nattel, S. (2002). "New ideas about atrial fibrillation 50 years on." Nature **415**(6868): 219-226.

Nattel, S., et al. (2003). Properties, Expression and Potential Roles of Cardiac K+ Channel Accessory Subunits: MinK, MiRPs, KChIP, and KChAP. J. Membrane Biol **194**: 141–152.

Nelson, M. E., et al. (2001). "Functional properties of human nicotinic AChRs expressed by IMR-32 neuroblastoma cells resemble those of alpha3beta4 AChRs expressed in permanently transfected HEK cells." J Gen Physiol **118**(5): 563-582.

Nury, H., et al. (2010). "One-microsecond molecular dynamics simulation of channel gating in a nicotinic receptor homologue." Proc Natl Acad Sci U S A **107**(14): 6275-6280.

Oh, S., et al. (2011). "Botulinum toxin injection in epicardial autonomic ganglia temporarily suppresses vagally mediated atrial fibrillation." Circ Arrhythm Electrophysiol **4**(4): 560-565.

Olson, T. M., et al. (2005). "Sodium channel mutations and susceptibility to heart failure and atrial fibrillation." JAMA **293**(4): 447-454.

Olson, T. M., et al. (2006). "Kv1.5 channelopathy due to KCNA5 loss-of-function mutation causes human atrial fibrillation." Hum Mol Genet **15**(14): 2185-2191.

Papke, R. L. (1993). "The kinetic properties of neuronal nicotinic receptors: genetic basis of functional diversity." Prog Neurobiol **41**(4): 509-531.

Parker, M. J., et al. (2001). "Determinants of agonist binding affinity on neuronal nicotinic receptor beta subunits." J Pharmacol Exp Ther **299**(1): 385-391.

Pourrier, M., et al. (2003). "Properties, expression and potential roles of cardiac K+ channel accessory subunits: MinK, MiRPs, KChIP, and KChAP." J Membr Biol **194**(3): 141-152.

Psaty, B. M., et al. (1997). "Incidence of and risk factors for atrial fibrillation in older adults." Circulation **96**(7): 2455-2461.

Purohit, P., et al. (2007). "A stepwise mechanism for acetylcholine receptor channel gating." Nature **446**(7138): 930-933.

Reitstetter, R., et al. (1999). "Dependence of nicotinic acetylcholine receptor recovery from desensitization on the duration of agonist exposure." J Pharmacol Exp Ther **289**(2): 656-660.

Roberts, J. D. and M. H. Gollob (2010). "Impact of genetic discoveries on the classification of lone atrial fibrillation." J Am Coll Cardiol **55**(8): 705-712.

Rust, G., et al. (1994). "Expression of neuronal nicotinic acetylcholine receptor subunit genes in the rat autonomic nervous system." Eur J Neurosci **6**(3): 478-485.

Sampson, K. J., et al. (2008). "Adrenergic regulation of a key cardiac potassium channel can contribute to atrial fibrillation: evidence from an I Ks transgenic mouse." J Physiol **586**(2): 627-637.

Scanavacca, M., et al. (2006). "Selective atrial vagal denervation guided by evoked vagal reflex to treat patients with paroxysmal atrial fibrillation." Circulation **114**(9): 876-885.

Scanavacca, M. and E. Sosa (2009). "Catheter ablation techniques for selective cardiac autonomic denervation to treat patients with paroxysmal atrial fibrillation." Heart Rhythm **6**(9): 1265-1266.

Severance, E. G. and R. H. Yolken (2007). "Lack of RIC-3 congruence with beta2 subunit-containing nicotinic acetylcholine receptors in bipolar disorder." Neuroscience **148**(2): 454-460.

Shteingauz, A., et al. (2009). "The BTB-MATH protein BATH-42 interacts with RIC-3 to regulate maturation of nicotinic acetylcholine receptors." J Cell Sci **122**(Pt 6): 807-812.

Skok, V. I. (2002). "Nicotinic acetylcholine receptors in autonomic ganglia." Auton Neurosci **97**(1): 1-11.

Smeets, J. L., et al. (1986). "The wavelength of the cardiac impulse and reentrant arrhythmias in isolated rabbit atrium. The role of heart rate, autonomic transmitters, temperature, and potassium." Circ Res **58**(1): 96-108.

Stafford, P. J., et al. (1991). "Quantitative analysis of signal-averaged P waves in idiopathic paroxysmal atrial fibrillation." Am J Cardiol **68**(8): 751-755.

Taly, A., et al. (2009). "Nicotinic receptors: allosteric transitions and therapeutic targets in the nervous system." Nat Rev Drug Discov **8**: 733–750.

Tamargo, J. and E. Delpon (2009). "Vagal stimulation and atrial electrical remodeling." Rev Esp Cardiol **62**(7): 729-732.

Thibodeau, I. L., et al. (2010). "Paradigm of genetic mosaicism and lone atrial fibrillation: physiological characterization of a connexin 43-deletion mutant identified from atrial tissue." Circulation **122**(3): 236-244.

Thomas, P. and T. G. Smart (2005). "HEK293 cell line: a vehicle for the expression of recombinant proteins." J Pharmacol Toxicol Methods **51**(3): 187-200.

Thompson, A. J., et al. (2010). "The structural basis of function in Cys-loop receptors." Q Rev Biophys **43**(4): 449-499.

Treinin, M. (2008). "RIC-3 and nicotinic acetylcholine receptors: biogenesis, properties, and diversity." Biotechnol J **3**(12): 1539-1547.

Vallés, A. S., et al. (2012). “Chaperoning α7 neuronal nicotinic acetylcholine receptors.” Biochimica et Biophysica Acta **1818**:718–729.

Veenhuyzen, G. D., et al. (2004). "Atrial fibrillation." CMAJ **171**(7): 755-760.

Wang, N., et al. (2002). "Autonomic function in mice lacking alpha5 neuronal nicotinic acetylcholine receptor subunit." J Physiol **542**(Pt 2): 347-354.

Wang, N., et al. (2003). "Deficiency of nicotinic acetylcholine receptor beta 4 subunit causes autonomic cardiac and intestinal dysfunction." Mol Pharmacol **63**(3): 574-580.

Wang, Y., et al. (2009). "Mouse RIC-3, an endoplasmic reticulum chaperone, promotes assembly of the alpha7 acetylcholine receptor through a cytoplasmic coiled-coil domain." J Neurosci **29**(40): 12625-12635.

Weber, M., et al. (1975). "Regulation of binding properties of the nicotinic receptor protein by cholinergic ligands in membrane fragments from Torpedo marmorata." Proc Natl Acad Sci U S A **72**(9): 3443-3447.

Wells, J. L., Jr., et al. (1978). "Characterization of atrial fibrillation in man: studies following open heart surgery." Pacing Clin Electrophysiol **1**(4): 426-438.

Williams, M. E., et al. (2005). "Ric-3 promotes functional expression of the nicotinic acetylcholine receptor alpha7 subunit in mammalian cells." J Biol Chem **280**(2): 1257-1263.

Wolf, P. A., et al. (1991). "Atrial fibrillation as an independent risk factor for stroke: the Framingham Study." Stroke **22**(8):983-988.

Xu, W., et al. (1999a). "Megacystis, mydriasis, and ion channel defect in mice lacking the alpha3 neuronal nicotinic acetylcholine receptor." Proc Natl Acad Sci U S A **96**(10): 5746-5751.

Xu, W., et al. (1999b). "Multiorgan autonomic dysfunction in mice lacking the beta2 and the beta4 subunits of neuronal nicotinic acetylcholine receptors." J Neurosci **19**(21): 9298-9305.

Yamada, M., et al. (1998). "G protein regulation of potassium ion channels." Pharmacol Rev **50**(4): 723-760.

Yatani, A., et al. (1990). "Heart rate regulation by G proteins acting on the cardiac pacemaker channel." Science **249**(4973): 1163-1166.

Yeh, Y-H., et al. (2007). Vagal Atrial Fibrillation. Acta Cardiol Sin **23**: 1-12.

Zhang, J., et al. (1999). "Activation and Ca2+ permeation of stably transfected alpha3/beta4 neuronal nicotinic acetylcholine receptor." Mol Pharmacol **55**(6): 970-981.

Zhang, J., et al. (2013). "The structural mechanism of the Cys-loop receptor desensitization." Molecular Neurobiology **48** (1): 97-108.

Zimmermann, M. (2003). "Autonomic tone and atrial fibrillation." J Cardiovasc Electrophysiol **14**(6): 565-566.